

University of Massachusetts Medical School

eScholarship@UMMS

GSBS Student Publications

Graduate School of Biomedical Sciences

2013-12-01

Functional overlap among distinct G1/S inhibitory pathways allows robust G1 arrest by yeast mating pheromones


Patricia A. Pope

University of Massachusetts Medical School

Et al.

Let us know how access to this document benefits you.

Follow this and additional works at: https://escholarship.umassmed.edu/gsbs_sp

 Part of the [Cell Biology Commons](#), [Cellular and Molecular Physiology Commons](#), and the [Molecular Biology Commons](#)

Repository Citation

Pope PA, Pryciak PM. (2013). Functional overlap among distinct G1/S inhibitory pathways allows robust G1 arrest by yeast mating pheromones. GSBS Student Publications. <https://doi.org/10.1091/mbc.E13-07-0373>. Retrieved from https://escholarship.umassmed.edu/gsbs_sp/1844

This material is brought to you by eScholarship@UMMS. It has been accepted for inclusion in GSBS Student Publications by an authorized administrator of eScholarship@UMMS. For more information, please contact Lisa.Palmer@umassmed.edu.

Functional overlap among distinct G1/S inhibitory pathways allows robust G1 arrest by yeast mating pheromones

Patricia A. Pope and Peter M. Pryciak

Department of Biochemistry and Molecular Pharmacology, University of Massachusetts Medical School, Worcester, MA 01605

ABSTRACT In budding yeast, mating pheromones arrest the cell cycle in G1 phase via a pheromone-activated Cdk-inhibitor (CKI) protein, Far1. Alternate pathways must also exist, however, because deleting the cyclin *CLN2* restores pheromone arrest to *far1Δ* cells. Here we probe whether these alternate pathways require the G1/S transcriptional repressors Whi5 and Stb1 or the CKI protein Sic1, whose metazoan analogues (Rb or p27) antagonize cell cycle entry. Removing Whi5 and Stb1 allows partial escape from G1 arrest in *far1Δ cln2Δ* cells, along with partial derepression of G1/S genes, which implies a repressor-independent route for inhibiting G1/S transcription. This route likely involves pheromone-induced degradation of Tec1, a transcriptional activator of the cyclin *CLN1*, because Tec1 stabilization also causes partial G1 escape in *far1Δ cln2Δ* cells, and this is additive with Whi5/Stb1 removal. Deleting *SIC1* alone strongly disrupts Far1-independent G1 arrest, revealing that inhibition of B-type cyclin-Cdk activity can empower weak arrest pathways. Of interest, although *far1Δ cln2Δ sic1Δ* cells escaped G1 arrest, they lost viability during pheromone exposure, indicating that G1 exit is deleterious if the arrest signal remains active. Overall our findings illustrate how multiple distinct G1/S-braking mechanisms help to prevent premature cell cycle commitment and ensure a robust signal-induced G1 arrest.

Monitoring Editor

Daniel J. Lew
Duke University

Received: Jul 9, 2013

Revised: Sep 23, 2013

Accepted: Sep 24, 2013

INTRODUCTION

Cell cycle progression in all organisms is regulated by both internal and external cues. In eukaryotes, the G1 phase of the cell cycle provides a critical period in which cells monitor whether conditions are appropriate for entry into a new division cycle (Morgan, 2007). Signals that control this decision include positive and negative growth factors, differentiation triggers, nutrient levels, and environmental stresses. These regulatory signals either promote or prevent the transition from a stable G1 state to a new round of DNA synthesis and mitosis. Often, cells become insensitive to these regulatory

signals once they initiate the G1/S transition, establishing a cell cycle commitment phenomenon known as Start in yeast and the Restriction Point in animal cells (Hartwell *et al.*, 1974; Pardee, 1974; Cross, 1995; Blagosklonny and Pardee, 2002). Accordingly, signals that influence cell cycle entry generally affect the molecular machinery that controls the G1/S transition. In all eukaryotes cell cycle transitions are promoted by cyclin-dependent kinases (Cdks), as well as by coordinate changes in gene expression, and these promoting factors are often held in check by inhibitory molecules to ensure that cell cycle progression is carefully controlled (Morgan, 2007). The overall architecture of the G1/S regulatory network is strongly conserved throughout eukaryotes, although some of the individual components may have evolved separately in yeasts versus animals (Cross *et al.*, 2011).

In the budding yeast *Saccharomyces cerevisiae*, a single Cdk, Cdc28, associates with nine different cyclins that help drive distinct cell cycle events (Bloom and Cross, 2007). The transition from G1 to S phase is predominantly controlled by the G1 cyclin Cln3 along with two G1/S cyclins, Cln1 and Cln2, whereas the subsequent events of DNA synthesis and mitosis (in S and M phases) are driven

This article was published online ahead of print in MBcC in Press (<http://www.molbiolcell.org/cgi/doi/10.1091/mbc.E13-07-0373>) on October 2, 2013.

Address correspondence to: Peter M. Pryciak (peter.pryciak@umassmed.edu).

Abbreviations used: Cdk, cyclin-dependent kinase; CKI, Cdk inhibitor; MAPK, mitogen-activated protein kinase; MBF, MluI-box binding factor; RT-qPCR, real-time quantitative PCR; SBF, Swi4/6-box binding factor.

© 2013 Pope and Pryciak. This article is distributed by The American Society for Cell Biology under license from the author(s). Two months after publication it is available to the public under an Attribution-NonCommercial-Share Alike 3.0 Unported Creative Commons License (<http://creativecommons.org/licenses/by-nc-sa/3.0>).

"ASCB®," "The American Society for Cell Biology®," and "Molecular Biology of the Cell®" are registered trademarks of The American Society of Cell Biology.

by six B-type cyclins (Clb1–Clb6). The decision of yeast cells to enter a new cell cycle can be profoundly influenced by the presence of an external cue known as mating pheromone, which promotes fusion of two haploid mating partner cells (Hartwell, 1973). During this mating reaction, pheromone activates an intracellular signaling pathway that arrests the cell cycle in G1 phase, before Start (Dohman and Thorner, 2001; Bardwell, 2005). An important factor in this G1 arrest pathway is the protein Far1, as *far1Δ* cells do not arrest in response to pheromone (Chang and Herskowitz, 1992). Far1 is believed to be a Cdk inhibitor (CKI) protein that blocks the activity of Cln-Cdc28 complexes and thereby prevents progression through Start (Peter *et al.*, 1993; Peter and Herskowitz, 1994; Tyers and Futcher, 1993; Jeoung *et al.*, 1998), although some findings conflict with this interpretation (Gartner *et al.*, 1998). Of note, however, in some circumstances Far1 is dispensable for G1 arrest. For example, removing the G1/S cyclin Cln2 from *far1Δ* cells (i.e., *far1Δ cln2Δ*) restores pheromone-induced G1 arrest (Chang and Herskowitz, 1992; Cherkasova *et al.*, 1999). Thus, even in the complete absence of Far1, pheromone signaling still can interfere with the ability of cells to pass Start and enter a new division cycle. Despite early recognition of this fact, the molecular mechanisms responsible for Far1-independent arrest remain obscure.

In this study, we probe the Far1-independent arrest mechanisms more closely in order to better understand how pheromone signaling regulates G1 arrest and provide more general insights into the multiplicity of factors that control cell cycle commitment decisions. We reasoned that pheromone arrest might involve known negative regulators of the G1/S transition that act as “brakes” to antagonize cell cycle entry in many eukaryotes (Morgan, 2007). One such negative regulator is the CKI protein Sic1 (Donovan *et al.*, 1994; Schwob *et al.*, 1994), which is functionally analogous to the mammalian CKI p27(Kip1) (Sherr and Roberts, 1999). During G1, these CKI proteins inhibit Cdks bound to B-type cyclins and thereby prevent premature entry into S phase. This inhibition is eventually released in late G1, when cyclin-Cdk activity reaches levels sufficient to target the CKI for degradation (Schwob *et al.*, 1994; Nash *et al.*, 2001; Cross *et al.*, 2007; Koivomagi *et al.*, 2011). Another mode of negative regulation involves transcriptional repression of genes expressed at the G1/S boundary. In animal cells, transcription of G1/S genes is activated by the E2F family of heterodimeric transcription factors and repressed by members of the retinoblastoma protein (Rb) family (Frolov and Dyson, 2004; van den Heuvel and Dyson, 2008). Yeast cells have an analogous system (Bahler, 2005; Wittenberg and Reed, 2005), in which G1/S transcription is driven by two heterodimeric transcription factors called SBF (Swi4-Swi6) and MBF (Mbp1-Swi6) and is inhibited in early G1 by the repressors Whi5 and Stb1 (Koch *et al.*, 1996; Costanzo *et al.*, 2003, 2004; de Bruin *et al.*, 2004, 2008; Bean *et al.*, 2005). These repressors block the activity of DNA-bound SBF and MBF in part by recruiting histone deacetylases (Huang *et al.*, 2009; Takahata *et al.*, 2009; Wang *et al.*, 2009); in late G1, they are dissociated via Cdk phosphorylation, allowing SBF/MBF-dependent transcription to ensue (Costanzo *et al.*, 2004; de Bruin *et al.*, 2004; Wagner *et al.*, 2009; Doncic *et al.*, 2011). Important targets of SBF and MBF include the G1/S cyclin genes *CLN1* and *CLN2*, which yields increased G1/S Cdk activity, thereby creating a positive feedback loop that helps to ensure a decisive G1/S transition (Cross and Tinkelenberg, 1991; Dirick and Nasmyth, 1991; Skotheim *et al.*, 2008). MBF/SBF-regulated genes are not expressed in pheromone-arrested cells, regardless of whether the arrest is Far1 dependent or independent (Wittenberg *et al.*, 1990; Cherkasova *et al.*, 1999), but it was

unclear whether this inhibited transcriptional state is a cause or an effect of G1 arrest.

Here we report that the CKI Sic1 is strongly required for arrest in the absence of Far1, although not when Far1 is present. The transcriptional repressors Whi5 and Stb1 also contribute to Far1-independent arrest, in a manner that is additive with the pheromone-induced degradation of Tec1, a transcriptional activator of *CLN1*. Our results reveal that multiple, functionally overlapping regulatory circuits control the sensitivity of the G1/S transition to the pheromone arrest signal. Collectively these multiple pathways provide robustness to the G1 arrest response, which may help to ensure that commitment to cell cycle entry occurs decisively rather than tentatively.

RESULTS

Studying Far1-independent G1 arrest using synchronous cultures

To test the contribution of various regulatory factors to pheromone arrest in both the presence and absence of Far1, we used synchronous cultures to measure the duration of G1 phase. The essential cell cycle gene *CDC20* was placed under control of a regulated promoter (P_{GAL1}), allowing cells to be arrested in M phase and then released in the presence or absence of pheromone. Cell cycle progression was monitored by measuring DNA content (using flow cytometry) and/or by scoring budding. This approach offered three useful features: 1) by measuring G1 duration, we could detect even relatively subtle and temporary effects on the G1/S transition; 2) by using synchronized cells, we could readily assess the uniformity of phenotypes; and 3) we could distinguish specific effects of pheromone on G1 arrest from effects on other cell cycle stages or cell viability (which will become important later).

In this experimental context (Figure 1A), most cells finish mitosis and enter G1 (i.e., 1C DNA) by 30–60 min after release from the M-phase block and then begin a new round of DNA synthesis roughly 30 min later (at 90 min). If pheromone is added, wild-type cells complete mitosis and then arrest in G1 (for >3 h). To compare multiple different strains and replicate experiments, we plotted the percentage of cells with 2C DNA content as a function of time (Figure 1B). Generally, M-phase-arrested cultures were 80–90% 2C, and by 60 min after release they had cycled back to G1 and were predominantly 1C (i.e., only 10–15% 2C). As expected, *far1Δ* cells did not arrest in G1 in the presence of pheromone (Figure 1B). (In addition, with or without pheromone, they showed an accelerated return to the 2C state after completing mitosis, consistent with previous findings that Far1 can alter the timing of the G1/S transition even without pheromone treatment; Alberghina *et al.*, 2004.) In contrast, when *far1Δ cln2Δ* cells were released in the presence of pheromone, they remained in G1 for an extended period (Figure 1B). This arrest was not as strong as in wild-type or *FAR1 cln2Δ* strains, as evidenced by the gradual increase in cells with 2C DNA content beginning at 120–150 min after release. Thus G1 arrest in the *far1Δ cln2Δ* cells is partially leaky, but pheromone clearly imposes a durable G1 delay that affects the majority of cells in the culture.

Separately, we tested how Far1 affects the window of time in which cells commit to a new division cycle (Figure 1C). After release of cultures from the M-phase block, aliquots were removed at intervals and treated with pheromone to test whether the cells could still arrest in G1 or were already committed to division. In wild-type and *cln2Δ* strains, cells transitioned from fully uncommitted (>95% arrest) to substantially committed (<65% arrest) between the 45- and 60-min time points. In the *far1Δ cln2Δ* strain, two differences were evident (Figure 1C). First, the commitment point occurred roughly

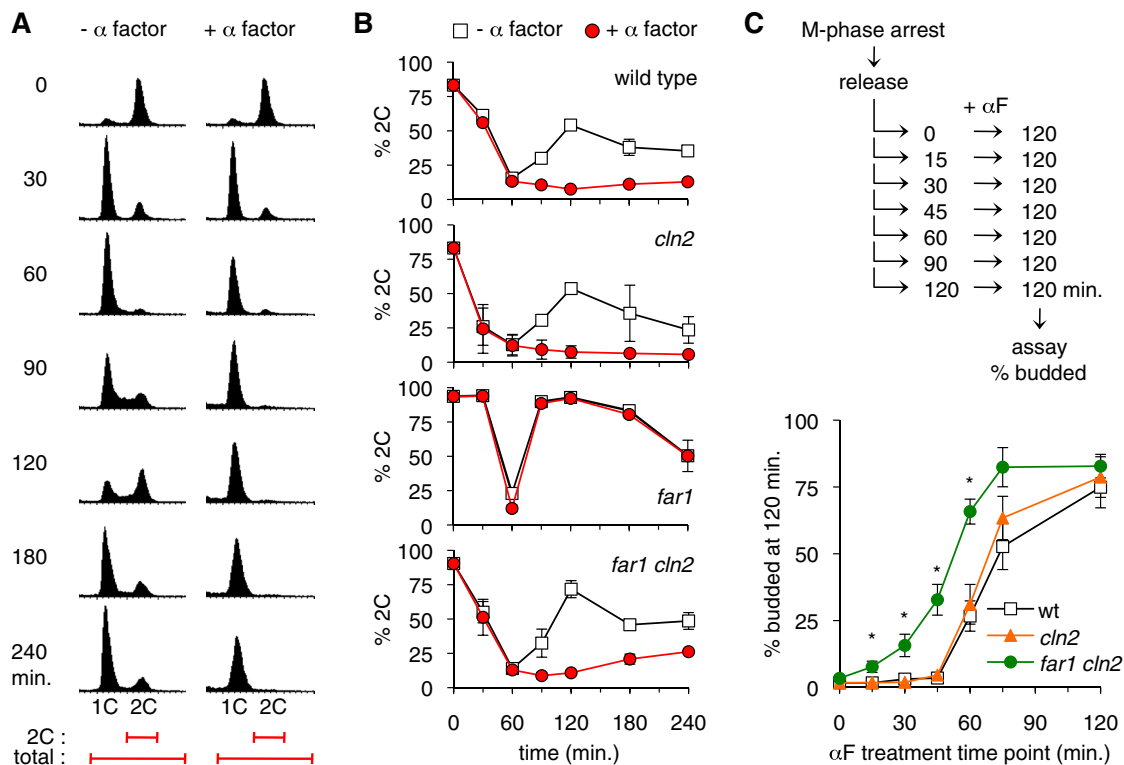


FIGURE 1: Far1-independent arrest and cell cycle commitment in synchronous cultures. (A) Example of synchronous cell cycle progression and G1 arrest. A P_{GAL1} - $CDC20$ strain was arrested in M phase (by transfer to glucose medium) and then released (by return to galactose medium) in the presence or absence of α factor. At the times indicated, DNA content of cells was assayed by flow cytometry. In each histogram, the horizontal axis represents fluorescence, and the vertical dimension shows the number of cells. Bottom, the range of fluorescence values used to calculate the proportion of cells with replicated DNA (percentage 2C) in subsequent figures. This example uses a $cln2\Delta$ strain (YPAP165). (B) The ability of α factor to halt cell cycle progression was analyzed for four strains, using the P_{GAL1} - $CDC20$ method described in A. Graphs show mean \pm range ($n = 2$) for wild-type and $far1\Delta$ or mean \pm SD ($n = 4$) for $cln2\Delta$ and $far1\Delta cln2\Delta$ strains. (C) Cell cycle commitment occurs earlier in the absence of Far1. After releasing P_{GAL1} - $CDC20$ cultures from the M-phase arrest, aliquots were removed at 15-min intervals and treated with pheromone. At 120 min, cells were scored for whether they had arrested in G1 (unbudded cells) or entered the cell cycle (budded). Graphs show mean \pm SEM ($n = 5$); asterisks indicate points where the difference between $far1\Delta cln2\Delta$ and $cln2\Delta$ was deemed statistically significant ($p < 0.025$; two-tailed unpaired t test).

15 min earlier, as judged by the time at which 50% of cells still arrest. Second, the transition was less sharp, as evidenced by a more gradual increase in the fraction of cells that could not arrest. Together these data indicate that Far1 makes the arrest mechanism more potent, as it allows pheromone to arrest cells that have advanced closer to Start, and also more robust, as the arrest is more uniform in $FAR1 cln2\Delta$ than $far1\Delta cln2\Delta$ cells. These findings complement a study in which the commitment point could be delayed by a stabilized form of Far1 (Doncic *et al.*, 2011). Nevertheless, despite these clear effects of Far1, our results show that a commitment point still exists in the absence of Far1, albeit one that is advanced so that the time window in which arrest can be imposed is more limited. In experiments to follow, the Far1-independent arrest phenotype in $far1\Delta cln2\Delta$ strains serves as sensitized setting in which to test the contribution of other factors that affect the G1/S transition.

Role of G1/S transcriptional repressors in G1 arrest

Previous studies found that expression of G1/S transcripts is inhibited in pheromone-arrested cells (Wittenberg *et al.*, 1990), even when the arrest is Far1 independent (Cherkasova *et al.*, 1999). Yet it was unclear whether this inhibition is a cause or a reflection of the G1 arrest. Hence, to determine whether Far1-independent arrest

relies on control of G1/S transcription, we probed the role of Whi5 and Stb1, the repressors of the G1/S transcription factors SBF and MBF. Deletion of $STB1$ alone produced no discernible change in either $FAR1 cln2\Delta$ or $far1\Delta cln2\Delta$ strains (Figure 2, A–D). Deletion of $WHI5$ had no effect in $FAR1 cln2\Delta$ cells (Figure 2A), but in $far1\Delta cln2\Delta$ cells (Figure 2C) it allowed a greater fraction of cells to escape G1 arrest (e.g., 38 vs. 24% 2C at 240 min). Assays using bud emergence as a marker of cell cycle progression yielded largely similar results, except that the escape phenotype caused by removing Whi5 was even more evident, and there was further enhancement when both Whi5 and Stb1 were removed (Figure 2D). Thus the transcriptional repressors contribute to Far1-independent G1 arrest. Despite these effects, the escape phenotypes were only partial, in that pheromone still imposed a significant G1 delay in the majority of cells.

We also tested the role of Mbp1, which is the DNA-binding component of the MBF heterodimer (Bahler, 2005). Although Mbp1 is required for transcriptional activation by MBF, it is also required for full repression of MBF-bound genes (Koch *et al.*, 1993; Bean *et al.*, 2005; de Bruin *et al.*, 2006). We found that removing Mbp1 from $far1\Delta cln2\Delta$ cells caused a more complete arrest rather than increased escape (Figure 2E), suggesting that either its role as an

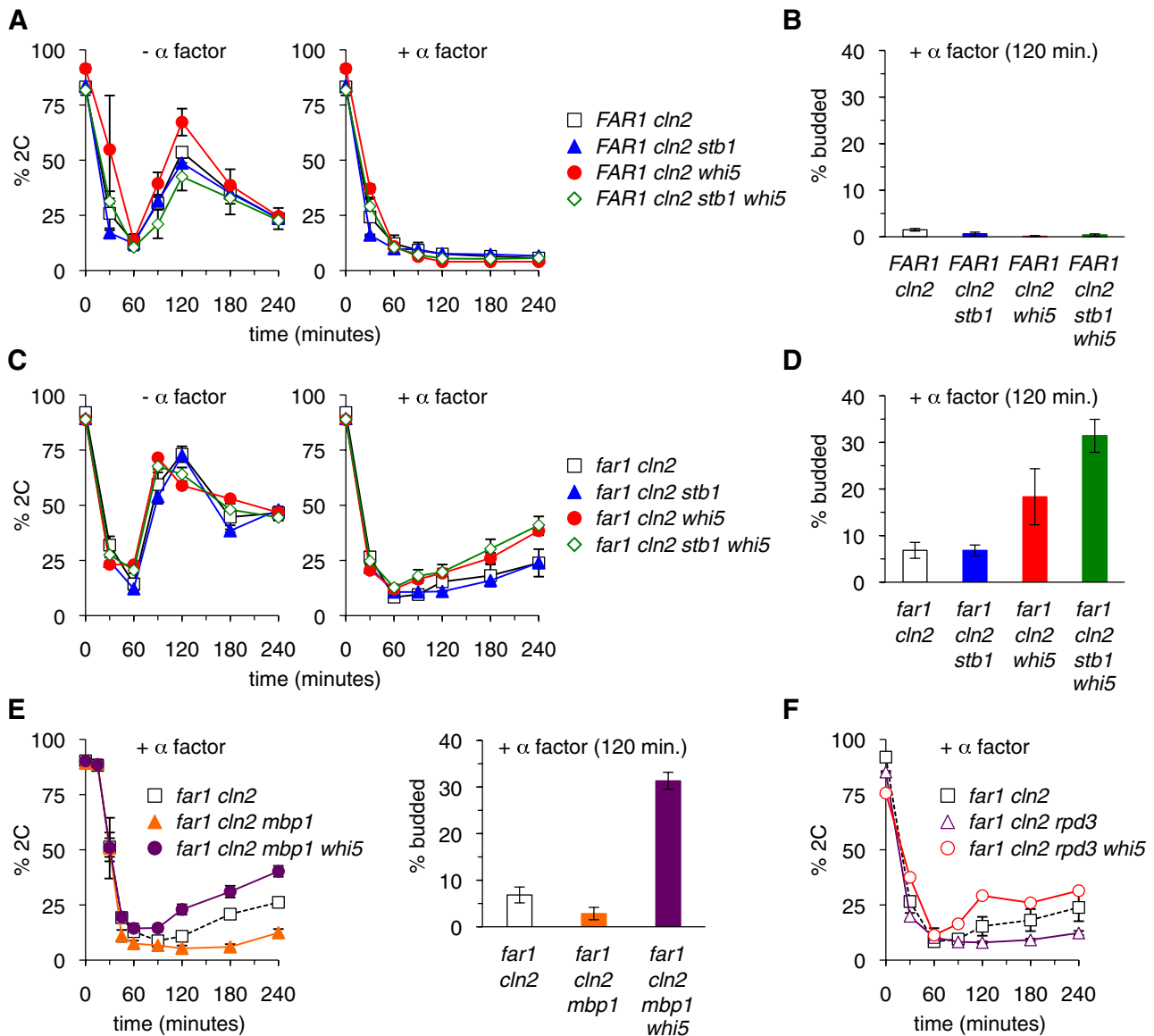


FIGURE 2: Partial role for transcriptional repressors in Far1-independent arrest. (A) Removal of Whi5 and/or Stb1 does not affect G1 arrest when Far1 is present. P_{GAL1} -*CDC20* strains in the *FAR1 cln2Δ* background were arrested in M phase and released in the presence or absence of pheromone. Cell cycle progression and G1 arrest were measured by the flow cytometry assay of DNA content. Graphs show mean \pm SEM ($n = 4-8$). (B) The strains in A were tested for G1 arrest by the budding assay. Budding was scored 120 min after release from M-phase arrest in the presence of α factor. Bars, mean \pm SEM ($n = 3-4$). (C) Removal of Whi5 partially compromises Far1-independent arrest. Cell cycle progression and G1 arrest were measured in *far1Δ cln2Δ* strains by the DNA assay. Graphs show mean \pm SEM ($n = 4-8$). (D) Strains from C were tested for G1 arrest by the budding assay as in B. Bars show mean \pm SEM ($n = 6$). (E) Mbp1 is not required for Far1-independent arrest or for the role of Whi5. G1 arrest was measured by the DNA (left) and budding (right) assays. Data points, mean \pm SEM ($n = 3$). (F) Rpd3 is not required for the role of Whi5. Graphs show mean \pm SEM ($n = 4$) for *far1Δ cln2Δ* and *far1Δ cln2Δ rpd3Δ* or mean \pm range ($n = 2$) for *far1Δ cln2Δ rpd3Δ whi5Δ*.

activator outweighs its role as a repressor in this setting or its removal allows stronger gene repression during pheromone treatment, possibly due to increased binding of SBF to MBF target genes (de Bruin *et al.*, 2006). Deleting *WHI5* from these *far1Δ cln2Δ mbp1Δ* cells allowed increased escape from G1 arrest (Figure 2E), with an especially strong difference (i.e., with vs. without Whi5), although the effect remained partial such that the majority of cells still arrested.

Whi5 and Stb1 repress transcription in part through the recruitment of the histone deacetylase Rpd3 (Huang *et al.*, 2009; Takahata

et al., 2009; Wang *et al.*, 2009). To determine whether the reduced arrest proficiency of the *far1Δ cln2Δ whi5Δ* strain was due to the loss of Rpd3 recruitment, we tested *far1Δ cln2Δ rpd3Δ* strains (Figure 2F). In fact, deletion of Rpd3 did not increase escape from G1 arrest and instead seemed to make G1 exit even slower, although this may reflect a slightly decreased growth rate of *rpd3Δ* mutants. Furthermore, Rpd3 is not required for the G1 arrest role of Whi5, because removing Whi5 from the *far1Δ cln2Δ rpd3Δ* strain still led to increased escape, indicating that the *whi5Δ* phenotype cannot be attributed solely to a defect in Rpd3 recruitment.

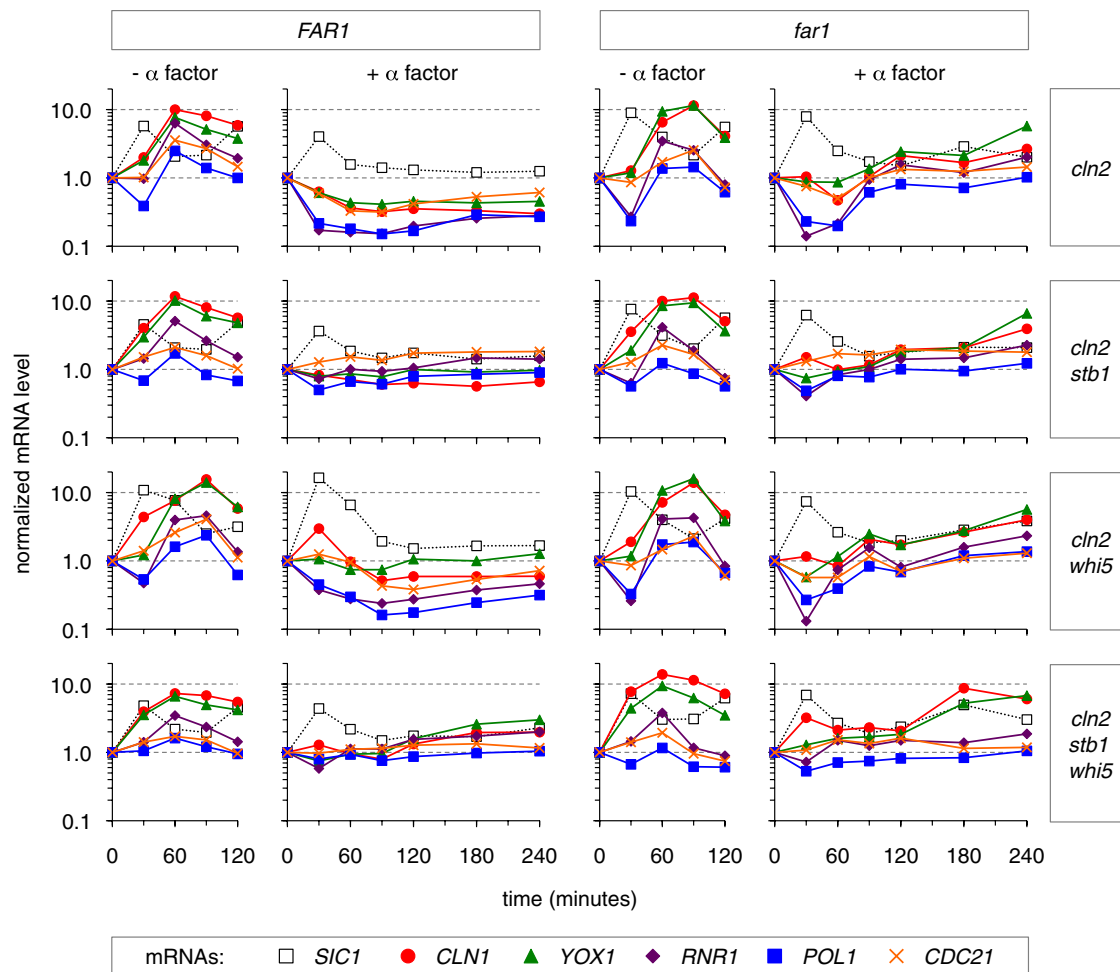


FIGURE 3: Effects of Far1, Whi5, and Stb1 on G1/S mRNA levels. The effects of Whi5 and Stb1 on G1/S transcript levels were measured in *FAR1 cln2Δ* (left) and *far1Δ cln2Δ* (right) backgrounds. P_{GAL1} -*CDC20* strains were arrested in M phase and released with or without α factor. At 30-min intervals, mRNA levels were measured by RT-qPCR (see *Materials and Methods*). Five G1/S transcripts (*CLN1*, *YOX1*, *RNR1*, *POL1*, and *CDC21*) and one M/G1 transcript (*SIC1*) were monitored. mRNA levels at each time point were plotted relative to the levels present in the M-phase–arrested cultures ($t = 0$). The drop in G1/S transcript levels from M phase ($t = 0$) to G1 ($t = 30$ min) was unexpected because these genes are not believed to be active during mitosis; this behavior might reflect imperfect synchronization in M phase, or it might indicate that maximal repression of these genes requires nuclear localization of Swi6 and DNA binding by SBF/MBF, which are inhibited by high Cdk activity in M phase (Sidorova *et al.*, 1995; Koch *et al.*, 1996; Queralt and Igual, 2003; Geymonat *et al.*, 2004). See Figure 4 for further analyses.

Collectively these results show that Whi5 and Stb1 are not required for the strong G1 arrest seen when Far1 is present, but they contribute to the weaker G1 arrest observed in cells that lack Far1. Even so, their removal from *far1Δ cln2Δ* cells causes only a partial defect in G1 arrest, indicating that pheromone signaling can still inhibit the G1/S transition in the absence of both Far1 and these transcriptional repressors.

Loss of repressors only partially derepresses transcription

We considered two possible explanations for why removing the transcriptional repressors did not fully eliminate G1 arrest in *far1Δ cln2Δ* cells: 1) pheromone signaling might still be able to inhibit G1/S transcription even without the repressors; and 2) the G1/S transcripts could be fully derepressed, but pheromone signaling might exert nontranscriptional effects that inhibit exit from G1. To test these possibilities, we analyzed G1/S transcript levels via real-time quantitative PCR (RT-qPCR). We chose five representative genes (*CLN1*, *YOX1*, *POL1*, *RNR1*, and *CDC21*) that are induced by

SBF and/or MBF at the G1/S transition (Bean *et al.*, 2005; de Bruin *et al.*, 2006; Eser *et al.*, 2011). For comparison, we also monitored a gene expressed at the earlier M/G1 boundary (*SIC1*). We first conducted single-time-course experiments for eight different strains, in which we measured transcript levels at numerous time points in synchronous cultures (Figure 3). Then we analyzed the most informative time points in multiple independent trials (Figure 4).

In cells released from mitosis without pheromone, the M/G1 and G1/S transcripts peaked at 30 and 60 min, respectively (Figure 3). This agrees with the timing of DNA synthesis and budding (which begin at 60–90 min). Adding pheromone prevented the G1/S peak in *FAR1 cln2Δ* cells, and instead these transcripts declined to a minimum at 60 min and remained low for up to 4 h (Figure 3). In the absence of Far1 (*far1Δ cln2Δ* cells), pheromone still inhibited the G1/S peak, but after 60 min these transcripts gradually increased, reaching levels that were higher than the corresponding *FAR1 cln2Δ* cells but below the peak levels in untreated cells. This gradual increase is consistent with the leaky arrest phenotype of *far1Δ cln2Δ*

cells. As expected for transcriptional repressors, removal of *Whi5* and/or *Stb1* allowed G1/S transcripts to start increasing earlier and/or to reach elevated levels in pheromone-treated cells. More specifically, the *stb1Δ* mutation seemed to reduce the pheromone-mediated decrease in all transcripts upon release from the mitotic block, whereas the *whi5Δ* mutation was more selective for specific transcripts. Nevertheless, in the absence of either repressor, or both simultaneously, pheromone still interfered with peak gene expression. These patterns of partial derepression were seen in both *FAR1 cln2Δ* and *far1Δ cln2Δ* backgrounds, although inhibition by pheromone was generally more potent and durable when *Far1* was present. Clearly, pheromone signaling can prevent peak G1/S transcription even without *Whi5* and *Stb1*.

For further analysis we performed multiple repetitions of each time course experiment and then measured mRNA levels at 60 min after release from M phase (Figure 4), as this was when expression peaked in the absence of pheromone. Without pheromone, G1/S transcripts reached roughly the same peak level in all strains (Figure 4), consistent with previous findings that *Whi5* and *Stb1* only slightly affect peak expression (Costanzo *et al.*, 2003, 2004; de Bruin *et al.*, 2004, 2008; Takahata *et al.*, 2009). However, derepression was clearly evident in the pheromone-treated samples, as G1/S transcripts were no longer fully repressed when *Whi5* and/or *Stb1* were absent. Of note, however, even in the absence of both *Whi5* and *Stb1*, G1/S transcript levels in pheromone-treated cells did not reach the maximum seen in untreated samples. Therefore inactivation of these repressors is not sufficient for full expression of G1/S transcripts, as pheromone signaling can still prevent their full expression. For several mRNAs the highest levels were seen in the *far1Δ cln2Δ whi5Δ* and *far1Δ cln2Δ stb1Δ whi5Δ* strains, which agrees with the finding that these strains have the strongest G1 escape phenotype, yet the ability of pheromone to prevent peak expression in these strains also agrees with the finding that even the strongest G1 escape phenotypes were partial.

The mRNA analyses revealed striking synergy between *Far1* and *Whi5* (Figure 4). That is, for several genes there was an additive effect of removing both proteins (i.e., *far1Δ cln2Δ whi5Δ*), whereas pheromone treatment could still exert a strong repressive effect if either one was present (i.e., *FAR1 cln2Δ whi5Δ* or *far1Δ cln2Δ WHI5*). Again, this correlates with the arrest behavior, in that removing *Whi5* caused a notable escape phenotype only when *Far1* was absent. By contrast, the derepression caused by removing *Stb1* was not further enhanced when *Far1* was also removed (compare *FAR1 cln2Δ stb1Δ* with *far1Δ cln2Δ stb1Δ*), and the additive relationship between *Far1* and *Whi5* did not require *Stb1* (compare *FAR1 cln2Δ stb1Δ whi5Δ* with *far1Δ cln2Δ stb1Δ whi5Δ*). Together these results suggest that *Far1* and *Whi5* contribute additively to transcriptional repression, with a corresponding additive effect on G1 arrest. Because *Far1* is believed to inhibit *Cln-Cdk* activity (Peter *et al.*, 1993; Peter and Herskowitz, 1994; Tyers and Futcher, 1993; Jeoung *et al.*, 1998), the finding that it contributes to transcriptional repression even in the absence of *Whi5* and *Stb1* suggests that *Cdk* activity promotes G1/S transcription by additional mechanisms distinct from repressor displacement (see *Discussion*).

The *CLN1* transcription factor *Tec1* antagonizes G1 arrest

One route by which pheromone might inhibit G1/S transcription could involve the ability of the pheromone-activated mitogen-activated protein kinase (MAPK) *Fus3* to trigger degradation of the transcription factor *Tec1* (Bao *et al.*, 2004; Bruckner *et al.*, 2004; Chou *et al.*, 2004). Because *Tec1* positively regulates *CLN1* expression

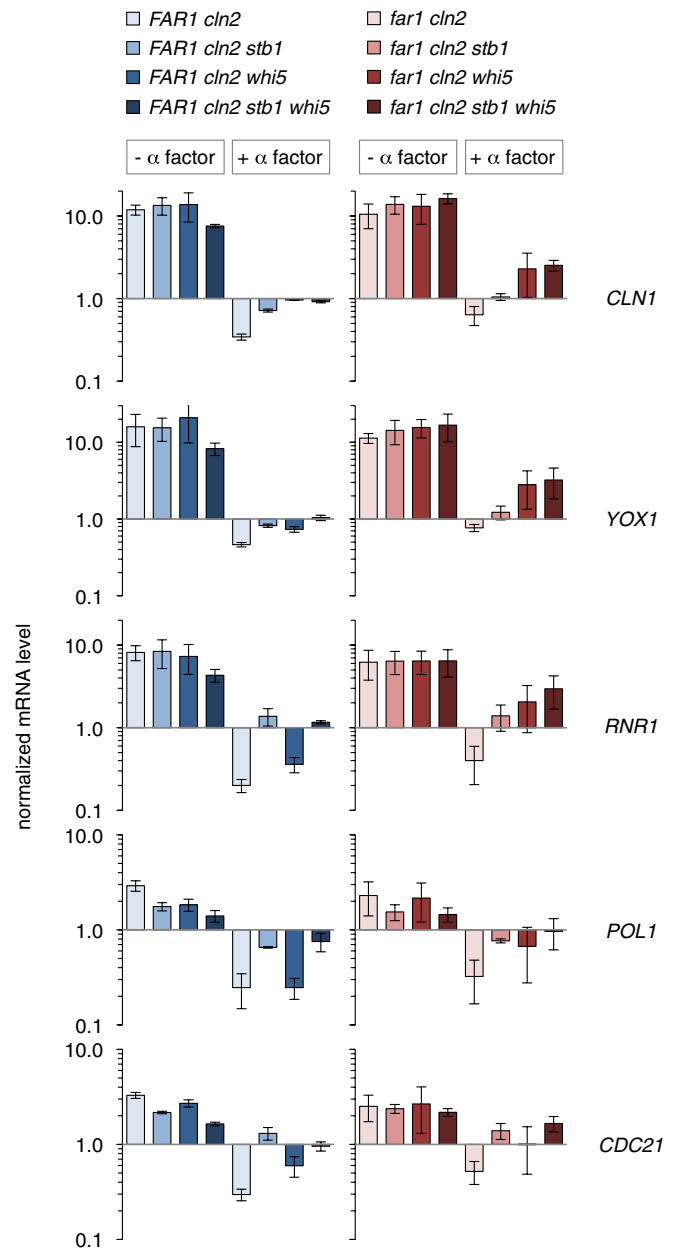


FIGURE 4: Loss of repressors only partially derepresses transcription. G1/S transcripts were assayed at a fixed time corresponding to the transition from G1 to S phase. The *P_{GAL1}-CDC20* arrest/release experiments shown in Figure 3 were repeated three times, and mRNA levels were measured before and 60 min after release in either the presence or absence of α factor. Bars, mRNA levels (mean \pm SD; $n = 3$) at the 60-min time points, expressed relative to the levels in the M-phase-arrested cells. The effects of *Whi5* and *Stb1* were compared in *FAR1 cln2Δ* (left) and *far1Δ cln2Δ* (right) backgrounds. Statistical analysis of all 120 pairwise comparisons, using the Benjamini–Hochberg false discovery rate method, is provided in Supplemental Table S1. The most pertinent points are 1) the inhibition by α factor is statistically significant ($q < 0.05$) for each of the eight individual genotypes and 2) the derepression due to removal of *Whi5*/*Stb1* is significant in most cases except for comparisons involving the *far1Δ cln2Δ whi5Δ* strain, for which greater variability prevents a firm conclusion, but the effect of *Whi5* is separately supported by comparing *far1Δ cln2Δ stb1Δ* with *far1Δ cln2Δ stb1Δ whi5Δ* (e.g., $q = 0.007$ for *CLN1* mRNA).

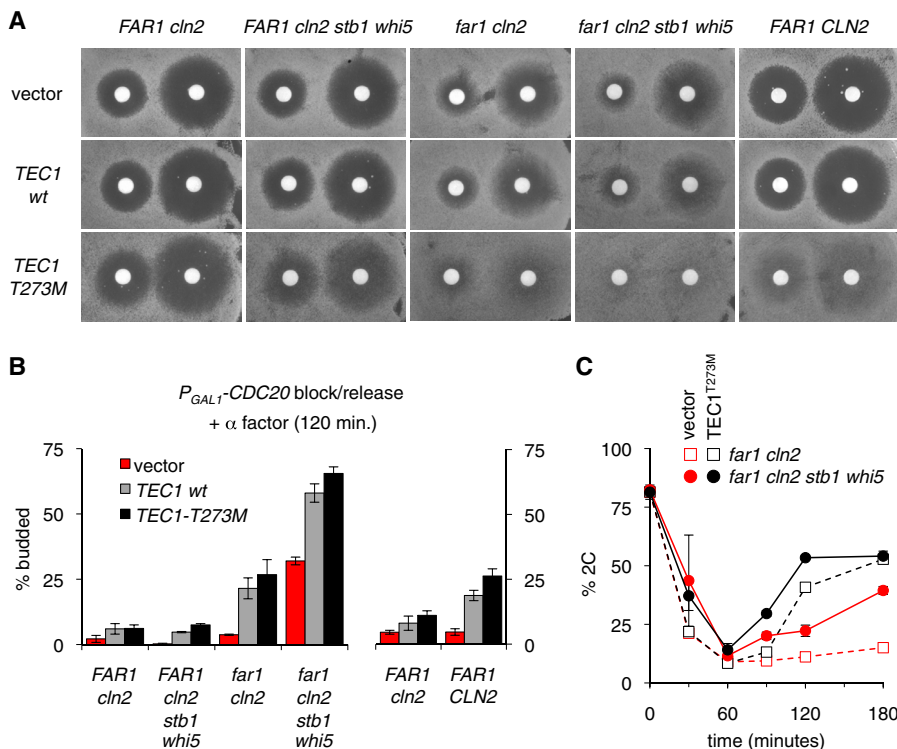


FIGURE 5: The *CLN1* transcription factor Tec1 antagonizes Far1-independent G1 arrest. (A) Empty vector or *TEC1* plasmids (pPP681, pPP4042, pPP4043) were introduced into the indicated strains (PPY1716, PPY1789, PPY1867, YPAP157, YPAP161). Cells were spread on selective media (SC –Ura), overlaid with filter disks containing 20 μ l of α factor (20 or 100 μ M), and then incubated at 30°C for 2 d. (B) Empty vector or *TEC1* plasmids (pPP680, pPP4050, pPP4051) were introduced into the indicated *P_{GAL1}-CDC20* strains (PPY2014, PPY2014, PPY2063, YPAP165, YPAP167, YPAP171). Cells were released from the mitotic block into medium containing α factor, and the percentage of cells that escaped G1 arrest was measured by scoring budding after 120 min. Bars, mean \pm range; the two strains at right ($n = 3$) were assayed together in a set of experiments separate from the four strains at left ($n = 2-5$). In each strain, differences between vector and *TEC1* (wild type and T273M) sets were ranked significant by a two-tailed unpaired *t* test (from left to right, $p = 0.008, 0.009, 0.014, 0.002, 0.005, 0.0002$). (C) *P_{GAL1}-CDC20* strains (PPY2014, YPAP171) contained empty vector or a *TEC1-T273M* plasmid (pPP680, pPP4051). Cells were released from the mitotic block into medium containing α factor, and DNA content was monitored at the indicated times. Graphs show mean \pm range of two separate experiments (some error bars are smaller than symbols).

(Madhani *et al.*, 1999; Bruckner *et al.*, 2004), its pheromone-induced degradation could indirectly dampen G1/S transcripts that are targets of Cln1-Cdc28 (Eser *et al.*, 2011), which might be especially consequential in *cln2 Δ* cells. To explore these notions, we first used halo assays to monitor how Tec1 affects growth arrest in both the presence and absence of Far1 (Figure 5A). We compared plasmids containing an extra copy of wild-type Tec1 or a mutant form, Tec1-T273M, which is resistant to pheromone-induced degradation (Bao *et al.*, 2004; Bruckner *et al.*, 2004; Chou *et al.*, 2004) and disrupts the ability of pheromone to inhibit *CLN1* expression (Bruckner *et al.*, 2004). We observed a gradual reduction in arrest proficiency as more regulatory pathways were inactivated. Specifically, the Tec1-T273M mutant caused only a mild arrest defect in *FAR1 cln2 Δ* cells (visible as a reduction in halo clarity and sharpness), but it caused a strong arrest defect in *far1 Δ cln2 Δ* cells, which was even stronger when Whi5/Stb1 were also absent (Figure 5A). By comparison, the extra copy of wild-type Tec1 had a milder effect in these assays. Overall the results suggest that pheromone inhibition of Tec1 activity becomes especially important when the Far1-dependent pathway is disrupted.

Related phenotypes were observed when cell cycle entry was analyzed in synchronous *P_{GAL1}-CDC20* cultures. Namely, extra Tec1 or stabilized Tec1-T273M caused only a mild escape from G1 arrest in *FAR1 cln2 Δ* cells but caused a substantial escape in *far1 Δ cln2 Δ* cells and had an additive effect with Whi5/Stb1 removal, such that the majority of *far1 Δ cln2 Δ stb1 Δ whi5 Δ* cells now escaped G1 arrest (Figure 5B). This additive effect was also clearly evident when the G1/S transition was monitored using DNA content (Figure 5C), for which we found that the degree of G1 escape was maximal upon the simultaneous removal of Whi5/Stb1 and stabilization of Tec1. It is not known why an extra copy of *TEC1* mimics *TEC1-T273M* more closely in synchronous assays (Figure 5B) than in halo assays (Figure 5A), but it is possible that the synchronization protocol imparts greater sensitivity to *TEC1* dose because of the transfer to glucose-free media, which increases expression of *TEC1* and Tec1-dependent genes (Cullen and Sprague, 2012). Nonetheless, the similar effects of both extra and stabilized Tec1 agree with the notion that pheromone arrest depends in part on blocking Tec1 accumulation. Taken together, our results indicate that Far1-independent arrest is promoted by two parallel pathways that act additively to reduce G1/S gene expression: Whi5/Stb1-mediated repression of SBF/MBF genes, and pheromone-triggered degradation of the *CLN1* transcription factor Tec1.

Sic1 plays a strong role in Far1-independent arrest

Finally, to assess how strongly Far1-independent pathways can contribute to arrest in an otherwise wild-type cell, we tested the same *TEC1* plasmids in a strain with intact copies of both *FAR1* and *CLN2*. Remarkably, the Tec1-T273M mutant caused much stronger pheromone resistance in *FAR1 CLN2* cells than in *FAR1 cln2 Δ* cells (Figure 5, A, leftmost vs. rightmost columns, and B, right). Thus the same pathway can promote arrest in both *far1 Δ cln2 Δ* cells and wild-type cells. In addition, these results reveal an interesting parallel between Far1-dependent and Far1-independent pathways, as the pheromone resistance phenotype of either *far1 Δ* or *TEC1-T273M* is suppressed by removing Cln2.

Another regulator of the G1/S transition is the protein Sic1, a CKI that inhibits S-phase cyclin-Cdks during early G1 and is inactivated in late G1 via phosphorylation by G1/S cyclin-Cdks. Because of its role as an antagonist of the G1/S transition, we tested whether Sic1 is involved in the Far1-independent arrest by pheromone (Figure 6). (These experiments exclusively used the budding assay because the *sic1 Δ* mutation caused extremely broad DNA flow cytometry profiles in *P_{GAL1}-CDC20* strains, which obscured the analysis.) Indeed, although deleting *SIC1* had no effect on G1 arrest when Far1 was present (Figure 6A), it had a substantial effect on Far1-independent arrest (Figure 6B). That is, in *far1 Δ cln2 Δ sic1 Δ* cells the ability of

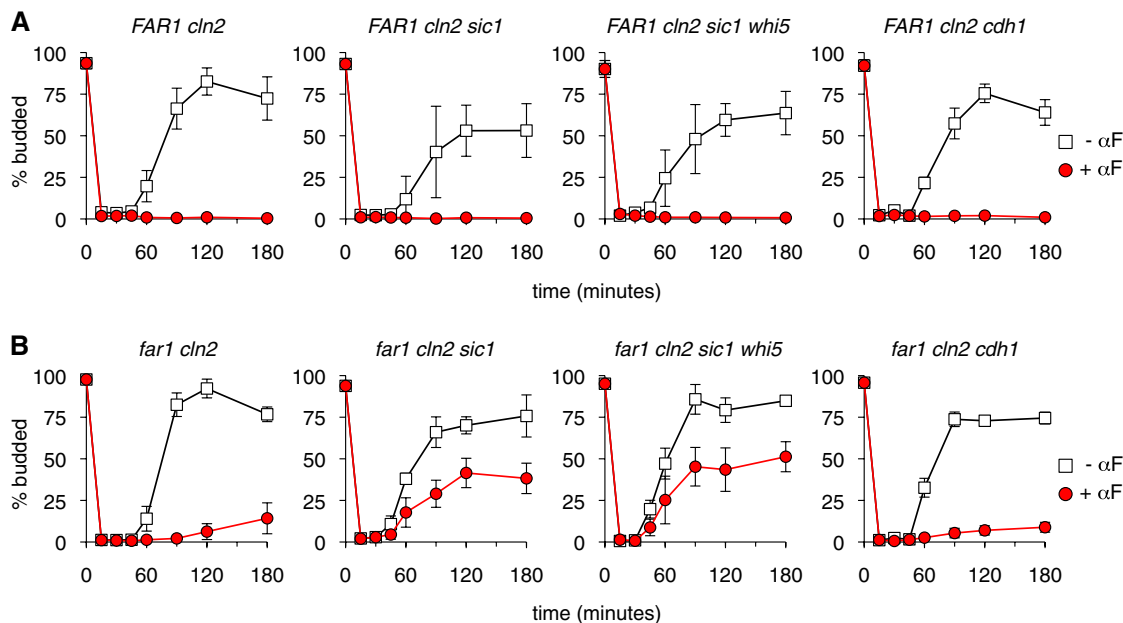


FIGURE 6: Sic1 plays a strong role in Far1-independent arrest. P_{GAL1} - $CDC20$ strains of the indicated genotypes were synchronized and then released into the presence or absence of α factor (α F). Cell cycle progression and G1 arrest was assayed by budding. (A, B) Results in the $FAR1$ $cln2\Delta$ and $far1\Delta$ $cln2\Delta$ backgrounds, respectively. All graphs show the mean \pm SD ($n = 4$ –6). Note that $far1\Delta$ $cln2\Delta$ $cdh1\Delta$ strains showed phenotypic heterogeneity that was isolate dependent. Specifically, we tested 12 isolates: six P_{GAL1} - $CDC20$ derivatives from each of two independent $far1\Delta$ $cln2\Delta$ $cdh1\Delta$ strains. The results shown are an average of three strains (YPAP242, 244, 245) that displayed the majority phenotype seen in 10 of 12 isolates. In two of 12 isolates, both derived from the same initial $far1\Delta$ $cln2\Delta$ $cdh1\Delta$ parent strain, we observed a notable escape phenotype (e.g., for YPAP243, ~40% budded cells after 120–180 min in α factor). The reason for this heterogeneity is unknown, but the observation of the escape phenotype in only a minority of derivatives (2/6) of one parent strain and in no derivatives (0/6) of the other suggests that a rare enhancer mutation may be responsible.

pheromone to impose a G1 arrest was strongly disrupted, although it was not eliminated. The residual arrest was not eliminated by further deletion of *WHI5* (Figure 6B), and hence we saw no evidence for synergy between Sic1 and Whi5. Furthermore, removing both Sic1 and Whi5 in a $FAR1$ background had no phenotype (Figure 6A). Thus removing any two antagonists of the G1/S transition is not sufficient to cause a G1 escape phenotype. Instead, this phenotype is only seen when combining $far1\Delta$ with either $whi5\Delta$ or $sic1\Delta$ mutations. We conclude that the G1/S-braking mechanism provided by Sic1 allows pheromone to activate a weakened G1 arrest response when Far1 is absent.

For comparison to the findings with Sic1, we tested another antagonist of S- and M-phase cyclins, namely, the APC component Cdh1, which inhibits accumulation of B-type cyclins during G1 (Visintin *et al.*, 1997; Morgan, 2007). We found that removal of Cdh1 in the $far1\Delta$ $cln2\Delta$ background caused a negligible change in G1 escape (Figure 6B), although for unknown reasons we did observe an increased escape phenotype in rare isolates (legend to Figure 6). Therefore these findings suggest that Far1-independent arrest depends more strongly on the inhibitor of Clb-Cdk activity (Sic1) than on the inhibitor of Clb protein accumulation (Cdh1). Note, however, that we cannot rule out the possibility that the absence of Cdh1 was suppressed in our experiments by ectopic expression of its functional relative, Cdc20, which enabled the cell synchronization protocol; for example, P_{GAL1} - $CDC20$ expression may limit accumulation of the B-type cyclin Clb2, which was shown previously to allow premature escape from pheromone arrest in a fraction of $cdh1$ (*hct1-3*) mutant cells (Schwab *et al.*, 1997).

G1 arrest failure can compromise cell viability

Although removing Sic1 allowed $far1\Delta$ $cln2\Delta$ cells to escape pheromone-induced G1 arrest more readily, it appeared to cause enhanced sensitivity to pheromone when growth arrest was measured by a long-term halo assay (Figure 7A). This paradox led us to consider the possibility that the failure of these cells to arrest in G1 causes reduced viability during continuous incubation with pheromone. Therefore we assayed cell viability in asynchronous cultures treated with pheromone for various times (Figure 7B). Wild-type strains maintained viability for several hours, but the $far1\Delta$ $cln2\Delta$ $sic1\Delta$ strain showed a clear loss of viability after only a short period (2–4 h). This reduced viability was not seen in the absence of pheromone (legend to Figure 7) or when either Far1 or Sic1 was present (i.e., $FAR1$ $cln2\Delta$ $sic1\Delta$ or $far1\Delta$ $cln2\Delta$ $SIC1$ strains), suggesting that it is not the presence or absence of either protein per se but rather the rapid escape from G1 that ultimately causes reduced viability in the $far1\Delta$ $cln2\Delta$ $sic1\Delta$ strain. Furthermore, simultaneous absence of both proteins was tolerated if strains retained *CLN2* (i.e., $far1\Delta$ $sic1\Delta$ strains; Figure 7C). Because Cln2 plays a prominent role in blocking pheromone response as cells pass Start (Oehlen and Cross, 1994; Strickfaden *et al.*, 2007), the combined results suggest that the observed inviability is due to cells exiting G1 without down-regulating pheromone signaling.

These implications were further corroborated by other experiments that did not involve Far1, Sic1, or Cln2. In particular, overproduction of the S-phase cyclin Clb5 can override G1 arrest by pheromone (Oehlen *et al.*, 1998), and a Cdk-resistant form of the signaling protein Ste5 (Ste5-8A) prevents pheromone response from being shut down in post-Start cells (Strickfaden *et al.*, 2007). The presence

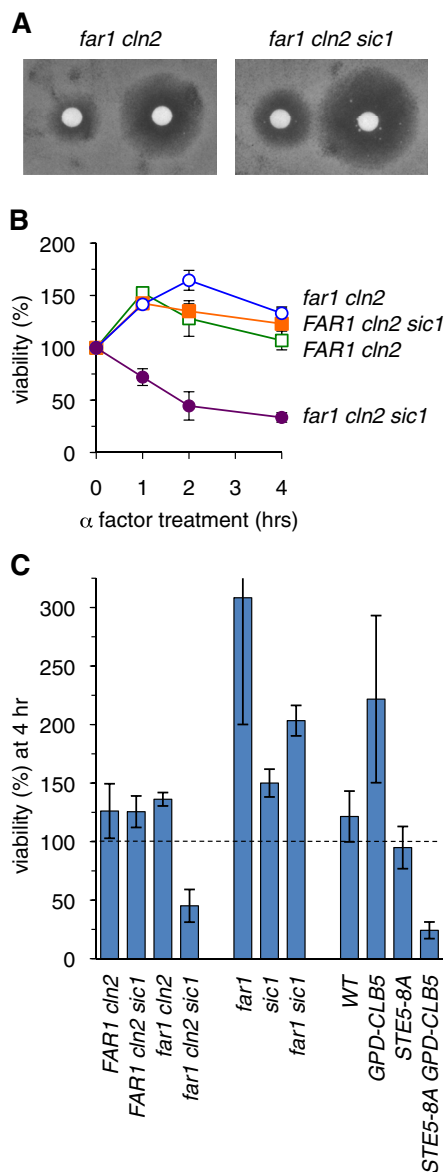


FIGURE 7: Failure to arrest in G1 causes loss of viability during pheromone exposure. (A) Removing Sic1 from *far1Δ cln2Δ* cells causes enhanced pheromone sensitivity when measured by a chronic growth arrest (halo) assay. Cells were spread on solid growth medium, overlaid with filter disks containing 20 μ l of α factor (20 or 100 μ M), and then incubated at 30°C for 2 d. (B) Pheromone treatment causes loss of viability in *far1Δ cln2Δ sic1Δ* cells. Asynchronous liquid cultures were incubated with pheromone for 1–4 h, and then cell viability was measured by plating on medium lacking pheromone and counting colony formation (see *Materials and Methods*). Viable cells at each time point were expressed relative to the number present before treatment ($t = 0$). Graphs show mean \pm range ($n = 2$). In parallel cultures incubated without pheromone, no differences in viability were observed among these strains (unpublished data). (C) Loss of cell viability is a consequence of escaping G1 arrest without inhibiting pheromone signaling. Asynchronous cultures were incubated with pheromone for 4 h, and viable cells were measured and expressed relative to the pretreated cultures ($t = 0$) as in B. Bars, mean \pm SD ($n = 4$). Strains that continue dividing in the presence of pheromone (e.g., *far1Δ*) show an increased number of viable cells at 4 h compared with pretreated culture. See the text for further explanation.

of both features together (i.e., *STE5-8A P_{GPD1}-CLB5* double mutants) caused cells to lose viability during pheromone exposure, whereas the single mutants did not (Figure 7C), arguing that inviability is a specific consequence of allowing pheromone signaling to continue in cells that escape the G1 arrest. Taken together, these findings illustrate the physiological importance of maintaining a robust G1 arrest in cells that are still transmitting the arrest signal. They also reveal that, under some circumstances, mutations that compromise G1 arrest would not be identified using only a growth arrest assay (see *Discussion*).

DISCUSSION

In this study we sought to increase our understanding of the mechanisms that yeast cells use to activate G1 arrest in response to extracellular mating pheromones. Previous findings indicate that this arrest does not absolutely require the pheromone-activated CKI Far1, because removal of Cln2 restores pheromone arrest to *far1Δ* cells. Thus here we compared Far1-dependent and Far1-independent G1 arrest in terms of their molecular phenotypes and their dependence on other inhibitory factors. We found that Far1 is not absolutely required for establishing a commitment point at Start, but it lengthens the time window in which pheromone can block this commitment step. Far1 also makes the G1 arrest process less dependent on other antagonists of the G1/S transition, such as repressors of G1/S transcription and inhibitors of S- and M-phase Cdk activity. Conversely, these repressors and inhibitors are not absolutely required for G1 arrest, but they reduce the dependence on Far1. Thus G1 arrest is made robust by functional overlap among multiple distinct G1/S inhibitory pathways (Figure 8).

In many eukaryotes it is believed that inhibition of G1/S transcription by Rb-like repressors and inhibition of S- and M-phase Cdk activity by Cip/Kip-like CKIs are key factors that restrain cell cycle entry and thereby impose a G1 waiting period (Morgan, 2007). In this study we found that pheromone-induced G1 arrest in budding yeast can still be imposed in the absence of the transcriptional repressors

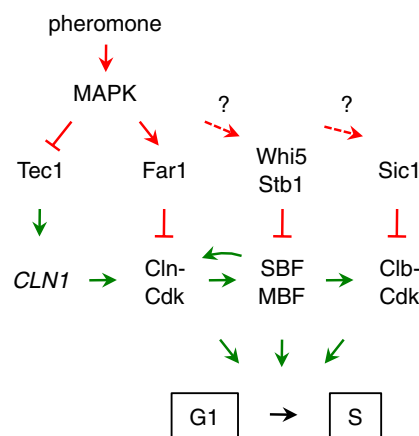


FIGURE 8: Simple illustration of multiple pathways contributing to pheromone arrest. Regulatory effects that inhibit or promote the G1/S transition are indicated in red or green, respectively. Dashed arrows with question marks emphasize that, although we found roles for Whi5/Stb1 and Sic1 in Far1-independent arrest, it is not known whether pheromone signaling enhances their inhibitory activity or simply depends on their constitutive effects. This simplified view is elaborated in greater detail in Supplemental Figure S1, which also includes a comparison of expected differences in wild-type, *far1Δ*, and *far1Δ cln2Δ* cells. See the text for further discussion.

Whi5/Stb1 or the CKI Sic1, or even both Whi5 and Sic1 simultaneously, but these negative factors become important for pheromone arrest in *far1Δ* cells. The existence of multiple braking mechanisms may help to prevent premature cell cycle entry when antiproliferative signals are present and expand the commitment decision period, perhaps by imposing a requirement that G1/S Cdk activity exceeds a sufficiently high threshold to counteract multiple antagonists. Such functional overlap, while in principle not required for a basic cell cycle, may increase the opportunities for regulatory control. Indeed, in animals there is evidence that Rb and CKIs can have additive effects in restraining proliferation of undifferentiated cells or redundant effects in terminally differentiated cells (Brugarolas *et al.*, 1998; Buttitta *et al.*, 2010; Wirt *et al.*, 2010).

It is noteworthy that removal of Whi5 and Stb1 was not sufficient for full expression of G1/S transcripts, despite evident derepression. Instead, we found that pheromone signaling inhibits expression of G1/S genes even in the absence of both repressors, similar to previous results in *whi5Δ* or *stb1Δ* single mutants (Costanzo *et al.*, 2004; de Bruin *et al.*, 2008). Because this inhibition was maximal when Far1 was present, it suggests that Cdk activity promotes full G1/S transcription by an additional route separate from its role in releasing repression by Whi5/Stb1, perhaps via direct phosphorylation of SBF and/or MBF. Indeed, Cdk sites have been identified in both Swi4 and Swi6, but direct evidence that Cdk phosphorylation of SBF/MBF enhances their activity is lacking (Sidorova *et al.*, 1995; Wijnen *et al.*, 2002); instead, mutational analyses suggest that Cdk phosphorylation of Swi6 or Whi5 acts redundantly to block repression (Costanzo *et al.*, 2004; de Bruin *et al.*, 2004; Wagner *et al.*, 2009). A further Cdk-regulated mechanism could affect the activity of SBF/MBF itself, an associated factor such as Msa1 (Ashe *et al.*, 2008), or a separate factor that cooperates with SBF/MBF such as Bck2 or Spt10 (Wijnen and Futcher, 1999; Eriksson *et al.*, 2011). The existence of such a mechanism also fits with the finding that stabilization of Tec1, which promotes *CLN1* expression and hence Cln1-Cdk activity, was able to increase escape from G1 arrest even when Whi5/Stb1 were already absent.

Although Whi5/Stb1 and Sic1 contribute to pheromone-induced arrest when Far1 is absent, it is not clear whether they are regulated by pheromone or function instead as constitutive inhibitors (see question marks in Figure 8). Because Sic1 can be phosphorylated and stabilized by another MAPK, Hog1 (Escote *et al.*, 2004), a similar effect could be exerted by the pheromone-regulated MAPK, Fus3. It is unlikely that the identical mechanism is used because the Hog1-phosphorylated form of Sic1 was absent in pheromone-arrested cells (Escote *et al.*, 2004), but another study did observe partial phosphorylation of the Sic1 N-terminus in pheromone-arrested cells (Koivomagi *et al.*, 2011), although the sites and responsible kinases are unknown. The effects of pheromone on G1/S transcription may be caused primarily by Far1-mediated inhibition of Cdk activity and MAPK-mediated degradation of Tec1, although it is conceivable that MAPK phosphorylation of SBF/MBF or Whi5/Stb1 provides another route for inhibition. Other pertinent mechanisms may include pheromone-induced reduction in Cln protein levels (Valdivieso *et al.*, 1993) or reductions in total protein synthesis rates (Goranov *et al.*, 2009; see question marks in Supplemental Figure S1), which may cause a rapid drop in the levels of short-lived cyclins and hence reduce cyclin-Cdk activity.

Which molecular targets can explain the escape phenotypes we obtained by inactivating inhibitory circuits in *far1Δ cln2Δ* cells? Ultimately, the key factor dictating whether cells can pass the G1/S transition despite the presence of pheromone may be acquisition of B-type Cdk activity, as pheromone cannot arrest cells in G1 if the

S-phase cyclin Clb5 is expressed from a strong foreign promoter (Oehlen *et al.*, 1998; Strickfaden *et al.*, 2007). This view can explain the effects of removing Sic1, which directly inhibits Clb5-Cdk activity (Schwob *et al.*, 1994). Furthermore, *CLB5* is an SBF-regulated gene, as are *CLN1* and *CLN2*, which engage in a positive feedback loop that enhances their own expression plus other SBF/MBF-dependent genes (Cross and Tinkelenberg, 1991; Dirick and Nasmyth, 1991; Skotheim *et al.*, 2008). Thus, in *far1Δ cln2Δ* cells, levels of *CLN1* and *CLB5* expression may determine whether sufficient Clb5-Cdk activity accumulates to pass Start, and hence their increased expression upon removal of Whi5/Stb1 and/or addition of stabilized Tec1 may cause the escape phenotype. In *far1Δ* single mutants, the presence of Cln2 may tip the balance in favor of Start by a mix of several effects: 1) it might simply increase the total cyclin dosage, equal to an extra copy of *CLN1*; 2) Cln2 might be a more effective promoter of Start than Cln1 (Tyers and Futcher, 1993), perhaps by providing greater Cdk activity toward key substrates like Whi5 and Sic1; and 3) Cln2 counteracts pheromone arrest by directly inhibiting pheromone signaling, and it does so more potently than does Cln1 (Oehlen and Cross, 1994; Strickfaden *et al.*, 2007). Thus, when Far1 is absent, the weaker Far1-independent arrest mechanisms can be overridden by Cln2 or genetic changes that increase Clb5-Cdk activity. When Far1 is present, the stronger inhibition of G1/S transcription may dampen Clb5 accumulation to a degree such that Sic1 is not needed for pheromone arrest. A comparison of these scenarios is illustrated in Supplemental Figure S1.

Finally, our findings reveal that robust G1 arrest is physiologically important, because if cell cycle entry occurs when cells are responding to pheromone, it can lead to irreversible, lethal effects. In particular, this was observed when *far1Δ cln2Δ sic1Δ* cells were exposed to pheromone; they were unable to arrest in G1, but they were nevertheless unable to divide and grow. Similar inviability was observed during pheromone treatment of *STE5–8A P_{GPD1}–CLB5* cells, in which G1 arrest is bypassed but signaling cannot be shut down. The cause of this inviability is not known, but ongoing studies suggest that pheromone signaling disrupts the function of the microtubule cytoskeleton during nuclear division (unpublished observations). Our findings clarify earlier results that implied that Sic1 was not required for Far1-independent arrest: namely, pheromone was able to arrest growth of *cln1Δ cln2Δ cln3Δ far1Δ sic1Δ* cells (Tyers, 1996). In retrospect, those cells may not have arrested in G1 but instead became inviable due to failed G1 arrest. These notions also illuminate an important consideration when analyzing other mutants for defects in pheromone-mediated arrest: if they allow slippage past the G1/S transition but do not prevent pheromone signaling, then the G1 arrest defect will not be noticeable by growth arrest assays. Hence it is conceivable that a distinct class of pheromone arrest mutants exists that would have gone undetected in prior genetic screens.

MATERIALS AND METHODS

Yeast strains and plasmids

Standard procedures were used for growth and genetic manipulation of yeast (Rothstein, 1991; Sherman, 2002). Yeast cultures were grown at 30°C. Strains and plasmids are listed in Tables 1 and 2, respectively; all yeast strains were derived from the W303 background (Thomas and Rothstein, 1989) and harbored the *bar1Δ* mutation to block α factor degradation. PCR-mediated gene targeting used methods described previously (Longtine *et al.*, 1998); selectable markers included antibiotic resistance genes (*kanMX6*, *natMX6*) and orthologues of biosynthesis genes from other yeasts (*Saccharomyces kluyveri HIS3*, *Candida glabrata TRP1*, *Kluyveromyces lactis URA3*). To ensure that genetic effects were reproducible, independently

Name	Relevant genotype ^a	Source	Name	Relevant genotype ^a	Source
PPY1716	MATa <i>bar1</i>	Zimmerman and Kellogg (2001)	YPAP138	MATa <i>bar1 cln2Δ::kanMX6 stb1Δ::natMX6 P_{GAL1}-CDC20::URA3^{KI}</i>	This study
PPY1748	MATa <i>bar1 STE5-8A</i>	Strickfaden et al. (2007)	YPAP141	MATa <i>bar1 far1Δ::ADE2 cln2Δ::kanMX6 stb1Δ::natMX6 P_{GAL1}-CDC20::URA3^{KI}</i>	This study
PPY1777	MATa <i>bar1 far1Δ::ADE2</i>	Strickfaden et al. (2007)	YPAP142	MATa <i>bar1 far1Δ::ADE2 cln2Δ::kanMX6 stb1Δ::natMX6 P_{GAL1}-CDC20::URA3^{KI}</i>	This study
PPY1789	MATa <i>bar1 far1Δ::ADE2 cln2Δ::kanMX6</i>	Strickfaden et al. (2007)	YPAP143	MATa <i>bar1 far1Δ::ADE2 cln2Δ::kanMX6 rpd3Δ::HIS3^{Sk} P_{GAL1}-CDC20::URA3^{KI}</i>	This study
PPY1867	MATa <i>bar1 cln2Δ::kanMX6</i>	This study	YPAP144	MATa <i>bar1 far1Δ::ADE2 cln2Δ::kanMX6 rpd3Δ::HIS3^{Sk} P_{GAL1}-CDC20::URA3^{KI}</i>	This study
PPY1913	MATa <i>bar1 HIS3::P_{GPD1}-CLB5</i>	Strickfaden et al. (2007)	YPAP151	MATa <i>bar1 far1Δ::ADE2 cln2Δ::kanMX6 whi5Δ::HIS3^{Sk} P_{GAL1}-CDC20::URA3^{KI}</i>	This study
PPY1918	MATa <i>bar1 STE5-8A HIS3::P_{GPD1}-CLB5</i>	Strickfaden et al. (2007)	YPAP152	MATa <i>bar1 far1Δ::ADE2 cln2Δ::kanMX6 whi5Δ::HIS3^{Sk} P_{GAL1}-CDC20::URA3^{KI}</i>	This study
PPY2013	MATa <i>bar1 far1Δ::ADE2 cln2Δ::kanMX6 P_{GAL1}-CDC20::URA3^{KI}</i>	This study	YPAP153	MATa <i>bar1 cln2Δ::kanMX6 whi5Δ::HIS3^{Sk} P_{GAL1}-CDC20::URA3^{KI}</i>	This study
PPY2014	MATa <i>bar1 far1Δ::ADE2 cln2Δ::kanMX6 P_{GAL1}-CDC20::URA3^{KI}</i>	This study	YPAP156	MATa <i>bar1 cln2Δ::kanMX6 whi5Δ::HIS3^{Sk} P_{GAL1}-CDC20::URA3^{KI}</i>	This study
PPY2019	MATa <i>bar1 far1Δ::ADE2 cln2Δ::kanMX6 mbp1Δ::TRP1^{Cg} P_{GAL1}-CDC20::URA3^{KI}</i>	This study	YPAP157	MATa <i>bar1 far1Δ::ADE2 cln2Δ::kanMX6 stb1Δ::natMX6 whi5Δ::HIS3^{Sk}</i>	This study
PPY2020	MATa <i>bar1 far1Δ::ADE2 cln2Δ::kanMX6 mbp1Δ::TRP1^{Cg} P_{GAL1}-CDC20::URA3^{KI}</i>	This study	YPAP161	MATa <i>bar1 cln2Δ::kanMX6 stb1Δ::natMX6 whi5Δ::HIS3^{Sk}</i>	This study
PPY2043	MATa <i>bar1 far1Δ::ADE2 cln2Δ::kanMX6 sic1Δ::TRP1^{Cg}</i>	This study	YPAP165	MATa <i>bar1 cln2Δ::kanMX6 P_{GAL1}-CDC20::URA3^{KI}</i>	This study
PPY2063	MATa <i>bar1 P_{GAL1}-CDC20::URA3^{KI}</i>	This study	YPAP166	MATa <i>bar1 cln2Δ::kanMX6 P_{GAL1}-CDC20::URA3^{KI}</i>	This study
PPY2064	MATa <i>bar1 P_{GAL1}-CDC20::URA3^{KI}</i>	This study	YPAP167	MATa <i>bar1 cln2Δ::kanMX6 stb1Δ::natMX6 whi5Δ::HIS3^{Sk} P_{GAL1}-CDC20::URA3^{KI}</i>	This study
PPY2068	MATa <i>bar1 far1Δ::ADE2 cln2Δ::kanMX6 sic1Δ::TRP1^{Cg} P_{GAL1}-CDC20::URA3^{KI}</i>	This study	YPAP168	MATa <i>bar1 cln2Δ::kanMX6 stb1Δ::natMX6 whi5Δ::HIS3^{Sk} P_{GAL1}-CDC20::URA3^{KI}</i>	This study
PPY2069	MATa <i>bar1 far1Δ::ADE2 cln2Δ::kanMX6 sic1Δ::TRP1^{Cg} P_{GAL1}-CDC20::URA3^{KI}</i>	This study	YPAP171	MATa <i>bar1 far1Δ::ADE2 cln2Δ::kanMX6 stb1Δ::natMX6 whi5Δ::HIS3^{Sk} P_{GAL1}-CDC20::URA3^{KI}</i>	This study
PPY2082	MATa <i>bar1 far1Δ::ADE2 P_{GAL1}-CDC20::URA3^{KI}</i>	This study	YPAP172	MATa <i>bar1 far1Δ::ADE2 cln2Δ::kanMX6 stb1Δ::natMX6 whi5Δ::HIS3^{Sk} P_{GAL1}-CDC20::URA3^{KI}</i>	This study
PPY2083	MATa <i>bar1 far1Δ::ADE2 P_{GAL1}-CDC20::URA3^{KI}</i>	This study	YPAP203	MATa <i>bar1 far1Δ::ADE2 cln2Δ::kanMX6 rpd3Δ::HIS3^{Sk} whi5Δ::TRP1^{Cg} P_{GAL1}-CDC20::URA3^{KI}</i>	This study
PPY2085	MATa <i>bar1 sic1Δ::TRP1^{Cg}</i>	This study	YPAP204	MATa <i>bar1 far1Δ::ADE2 cln2Δ::kanMX6 rpd3Δ::HIS3^{Sk} whi5Δ::TRP1^{Cg} P_{GAL1}-CDC20::URA3^{KI}</i>	This study
PPY2087	MATa <i>bar1 far1Δ::ADE2 sic1Δ::TRP1^{Cg}</i>	This study	YPAP208	MATa <i>bar1 cln2Δ::natMX6 sic1Δ::TRP1^{Cg}</i>	This study
PPY2090	MATa <i>bar1 far1Δ::ADE2 cln2Δ::kanMX6 mbp1Δ::TRP1^{Cg} whi5Δ::HIS3^{Sk} P_{GAL1}-CDC20::URA3^{KI}</i>	This study			
PPY2091	MATa <i>bar1 far1Δ::ADE2 cln2Δ::kanMX6 mbp1Δ::TRP1^{Cg} whi5Δ::HIS3^{Sk} P_{GAL1}-CDC20::URA3^{KI}</i>	This study			
PPY2128	MATa <i>bar1 far1Δ::ADE2 cln2Δ::kanMX6 mbp1Δ::TRP1^{Cg} whi5Δ::HIS3^{Sk} P_{GAL1}-CDC20::URA3^{KI}</i>	This study			
YPAP137	MATa <i>bar1 cln2Δ::kanMX6 stb1Δ::natMX6 P_{GAL1}-CDC20::URA3^{KI}</i>	This study			

TABLE 1: Yeast strains used in this study.

Continues

Name	Relevant genotype ^a	Source	Name	Relevant genotype ^a	Source
YPAP209	<i>MATa bar1 far1Δ::ADE2 cln2Δ::kanMX6 sic1Δ::TRP1^{Cg} whi5Δ::HIS3^{Sk} P_{GAL1}-CDC20::URA3^{Kl}</i>	This study	YPAP240	<i>MATa bar1 cln2Δ::kanMX6 cdh1Δ::HIS3^{Sk} P_{GAL1}-CDC20::URA3^{Kl}</i>	This study
YPAP210	<i>MATa bar1 far1Δ::ADE2 cln2Δ::kanMX6 sic1Δ::TRP1^{Cg} whi5Δ::HIS3^{Sk} P_{GAL1}-CDC20::URA3^{Kl}</i>	This study	YPAP241	<i>MATa bar1 cln2Δ::kanMX6 cdh1Δ::HIS3^{Sk} P_{GAL1}-CDC20::URA3^{Kl}</i>	This study
YPAP236	<i>MATa bar1 cln2Δ::natMX6 sic1Δ::TRP1^{Cg} P_{GAL1}-CDC20::URA3^{Kl}</i>	This study	YPAP242	<i>MATa bar1 far1Δ::ADE2 cln2Δ::kanMX6 cdh1Δ::HIS3^{Sk} P_{GAL1}- CDC20::URA3^{Kl}</i>	This study
YPAP237	<i>MATa bar1 cln2Δ::natMX6 sic1Δ::TRP1^{Cg} P_{GAL1}-CDC20::URA3^{Kl}</i>	This study	YPAP243	<i>MATa bar1 far1Δ::ADE2 cln2Δ::kanMX6 cdh1Δ::HIS3^{Sk} P_{GAL1}- CDC20::URA3^{Kl}</i>	This study
YPAP238	<i>MATa bar1 cln2Δ::natMX6 sic1Δ::TRP1^{Cg} whi5Δ::HIS3^{Sk} P_{GAL1}- CDC20::URA3^{Kl}</i>	This study	YPAP244	<i>MATa bar1 far1Δ::ADE2 cln2Δ::kanMX6 cdh1Δ::HIS3^{Sk} P_{GAL1}- CDC20::URA3^{Kl}</i>	This study
YPAP239	<i>MATa bar1 cln2Δ::natMX6 sic1Δ::TRP1^{Cg} whi5Δ::HIS3^{Sk} P_{GAL1}- CDC20::URA3^{Kl}</i>	This study	YPAP245	<i>MATa bar1 far1Δ::ADE2 cln2Δ::kanMX6 cdh1Δ::HIS3^{Sk} P_{GAL1}- CDC20::URA3^{Kl}</i>	This study

^aAll strains are in the W303 background (*ade2-1 his3-11,15 leu2-3112 trp1-1 ura3-1 can1*). In the *P_{GAL1}-CDC20* strains, a cassette containing the *URA3^{Kl}* marker and *GAL1* promoter is inserted in place of the *CDC20* promoter at the native *CDC20* locus.

TABLE 1: Yeast strains used in this study. Continued

derived strains of identical genotype were tested in parallel, and the combined results were averaged. For cell synchronization, the promoter of the essential cell cycle gene *CDC20* was replaced with a regulated promoter (*P_{GAL1}*) using a PCR-generated cassette marked with the *K. lactis URA3* gene (*URA3^{Kl}*).

Synchronous culture assays

To synchronize cell cultures, we placed the *CDC20* gene under control of the *GAL1* promoter (Cosma *et al.*, 2001; Bean *et al.*, 2005; Takahata *et al.*, 2009). These *P_{GAL1}-CDC20* strains were grown asynchronously in liquid YPGal medium (containing 2% galactose), and then cultures were arrested in M phase by pelleting and resuspending in YPD medium (2% glucose), followed by incubation for 3 h. Cultures were released from the M-phase block by two rounds of pelleting and washing in YPGal, resuspension in YPGal either with or without α factor (0.2 μ M), and incubation (with shaking) for 0–240 min. In experiments using *TEC1* plasmids, before the arrest in YPD and release in YPGal, cultures were grown overnight in synthetic media (SC –Leu, with 2% raffinose and 2% galactose) to maintain selection for *LEU2* plasmids.

Flow cytometry and budding assays

DNA content was measured by flow cytometry using previous methods (Haase and Reed, 2002; Strickfaden *et al.*, 2007). Briefly,

cell aliquots (0.5 ml) were harvested by centrifugation, resuspended in 0.3 ml water, fixed by addition of 0.7 ml of 100% ethanol, mixed by inversion, and incubated overnight at 4°C. Fixed cells were pelleted, washed once with water, resuspended in 0.5 ml of freshly prepared RNase solution (2 mg/ml RNase A in 50 mM Tris-HCl, pH 8.0, 15 mM NaCl), and incubated for 2 h at 36°C. They were then pelleted and resuspended in 0.2 ml of fresh proteinase solution (1 mg/ml proteinase K in 50 mM Tris-HCl, pH 8.0), incubated for 1 h at 36°C, then pelleted and resuspended in 0.5 ml of buffer (50 mM Tris-HCl, pH 7.5), and stored at 4°C. Before analysis, suspensions were sonicated (10 pulses with a microtip probe), and then 50 μ l was mixed with 1 ml of fresh Sytox Green solution (1 μ M in 50 mM Tris-HCl, pH 7.5), gently vortexed, and analyzed with a FACScan flow cytometer (BD, Franklin Lakes, NJ). For experiments that were directly compared with each other, a uniform range of fluorescence values was defined for both the 2C peak (generally 100–150 U) and the total (including 1C, 2C, and intermediate; generally 40–200 U), and then percentage 2C was calculated as $100\% \times 2C/\text{total}$.

To analyze cell cycle position by budding, cells aliquots (0.5 ml) were fixed by the addition of formaldehyde to 3.7% final concentration, incubated on a nutator (room temperature, 10 min), washed three times with phosphate-buffered saline (PBS), and resuspended in 500 μ l of PBS. Fixed cells were spotted onto glass slides and

Name	Alias	Description	Source
pPP680	pRS315	CEN/ARS LEU2 vector	Sikorski and Hieter (1989)
pPP681	pRS316	CEN/ARS URA3 vector	Sikorski and Hieter (1989)
pPP3025	pFA6a-URA3-PGAL1	PCR template for URA3 ^{Kl} -P _{GAL1} promoter insertion	This study
pPP4042	YCplac33-TEC1	CEN/ARS URA3 TEC1	Bao <i>et al.</i> (2004)
pPP4043	YCplac33-tec1-T273M	CEN/ARS URA3 TEC1-T273M	Bao <i>et al.</i> (2004)
pPP4050	pL-TEC1-WT	CEN/ARS LEU2 TEC1	This study
pPP4051	pL-TEC1-T273M	CEN/ARS LEU2 TEC1-T273M	This study

TABLE 2: Plasmids used in this study.

Primer name	Sequence (5' to 3')
CLN1-fw1	CTTTGGTTAGCGGCCAAAAC
CLN1-rev1	AGAAAGGCGTGAATACGAG
YOX1-up1	AAATAGGCGCTCATCCACAC
YOX1-dn1	ACGTTTTACGGGAGTCAAC
RNR1-up1	TCGAGGCTGCTTTAGAAACG
RNR1-dn1	GGCAACCAAGAAACAAGAGG
POL1-fw1	TGACATTTGCTCTGGTAGGC
POL1-rev1	CGGCTTATGCTCCTTTTCAC
CDC21-fw1	GGAACCCAGCTGATTTTGAC
CDC21-rev1	CGGATCCTTCTCCTTCTTTG
SIC1-fw1	CCAAAAGCCTTACAGAACC
SIC1-rev1	GAGAGGTCATACCCATGTTCC
ACT1-fw1	TTCCAGCCTTCTACGTTTCC
ACT1-rev1	CCAGCGTAAATTGGAACGAC

TABLE 3: Oligonucleotide primers used for RT-qPCR analysis.

viewed microscopically to score budded and unbudded cells; for each experimental condition, 200 cells were counted.

mRNA preparation and RT-qPCR analysis

RNA was prepared as described previously (de Bruin *et al.*, 2008) using an RNeasy Plus Mini Kit (74134; Qiagen, Valencia, CA). Cells ($\sim 5 \times 10^7$) were harvested by centrifugation and frozen in liquid nitrogen. Cell pellets were resuspended in 400 μ l of Qiagen RLT-plus buffer freshly supplemented with β -mercaptoethanol (10 μ l/ml of buffer) and transferred to a microcentrifuge tube. Approximately 400 μ l of acid-washed glass beads was added, and cells were lysed by vortexing (four cycles of 1 min, interspersed with rest periods of 3 min on ice). The tube was punctured at the bottom with a needle, placed in another tube, and centrifuged briefly (10 s) to transfer the lysate to the fresh tube. Then cell debris was removed by centrifugation (2 min, full speed). The supernatant was loaded onto Qiagen gDNA Eliminator columns, and then mRNA was prepared according to the manufacturer's instructions, diluted to equal concentrations (0.5 μ g/ μ l), and stored at -70°C . cDNA was synthesized from the RNA samples using a SuperScript VIL0 cDNA synthesis kit (11754; Invitrogen, Carlsbad, CA) as per the manufacturer's instructions, using ~ 2 μ g of RNA per reaction. Products were diluted to 2.5 ng/ μ l.

Quantitative real-time PCRs were performed using Power SYBR Green PCR Master Mix (4367659; Applied Biosystems, Foster City, CA). Reaction mixtures (15 μ l) contained 7.5 μ l of SYBR Green reaction mix, 2 μ l of primer mix (3 μ M each primer), 1 μ l of cDNA (2.5 ng), and 4.5 μ l of water. Reactions were performed in 96-well plates, in duplicate, using an Applied Biosystems StepOnePlus instrument. Preliminary trials using multiple primers for each gene were performed to identify primer sets with optimal properties (linearity of amplification) for use in all subsequent experiments. Primers are listed in Table 3. The $\Delta\Delta\text{C}_T$ method was used to convert real-time amplification kinetics into relative mRNA levels; *ACT1* mRNA served as the internal control.

Cell viability assays

Asynchronous cultures were treated with pheromone (0.2 μ M) for 1–4 h. Aliquots were collected before and after treatment, sonicated (seven pulses with a microtip probe), diluted in sterile PBS, spread

on solid synthetic medium, and incubated for 2 d. Viable colonies were counted and expressed as a percentage of the number obtained from equivalent aliquots of the initial, untreated cultures.

ACKNOWLEDGMENTS

We thank Hiten Madhani for *TEC1* plasmids, Nick Rhind for use of his flow cytometer, and Curt Wittenberg for mRNA/RT-qPCR protocols. This work was supported by a grant from the National Institutes of Health (GM57769) to P.M.P.

REFERENCES

- Alberghina L, Rossi RL, Querin L, Wanke V, Vanoni M (2004). A cell sizer network involving Cln3 and Far1 controls entrance into S phase in the mitotic cycle of budding yeast. *J Cell Biol* 167, 433–443.
- Ashe M, de Bruin RA, Kalashnikova T, McDonald WH, Yates JR 3rd, Wittenberg C (2008). The SBF- and MBF-associated protein Msa1 is required for proper timing of G1-specific transcription in *Saccharomyces cerevisiae*. *J Biol Chem* 283, 6040–6049.
- Bahler J (2005). Cell-cycle control of gene expression in budding and fission yeast. *Annu Rev Genet* 39, 69–94.
- Bao MZ, Schwartz MA, Cantin GT, Yates JR 3rd, Madhani HD (2004). Pheromone-dependent destruction of the Tec1 transcription factor is required for MAP kinase signaling specificity in yeast. *Cell* 119, 991–1000.
- Bardwell L (2005). A walk-through of the yeast mating pheromone response pathway. *Peptides* 26, 339–350.
- Bean JM, Siggia ED, Cross FR (2005). High functional overlap between Mlul cell-cycle box binding factor and Swi4/6 cell-cycle box binding factor in the G1/S transcriptional program in *Saccharomyces cerevisiae*. *Genetics* 171, 49–61.
- Blagosklonny MV, Pardee AB (2002). The restriction point of the cell cycle. *Cell Cycle* 1, 103–110.
- Bloom J, Cross FR (2007). Multiple levels of cyclin specificity in cell-cycle control. *Nat Rev Mol Cell Biol* 8, 149–160.
- Bruckner S, Kohler T, Braus GH, Heise B, Bolte M, Mosch HU (2004). Differential regulation of Tec1 by Fus3 and Kss1 confers signaling specificity in yeast development. *Curr Genet* 46, 331–342.
- Brugarolas J, Bronson RT, Jacks T (1998). p21 is a critical CDK2 regulator essential for proliferation control in Rb-deficient cells. *J Cell Biol* 141, 503–514.
- Buttitta LA, Katzaroff AJ, Edgar BA (2010). A robust cell cycle control mechanism limits E2F-induced proliferation of terminally differentiated cells in vivo. *J Cell Biol* 189, 981–996.
- Chang F, Herskowitz I (1992). Phosphorylation of FAR1 in response to alpha-factor: a possible requirement for cell-cycle arrest. *Mol Biol Cell* 3, 445–450.
- Cherkasova V, Lyons DM, Elion EA (1999). Fus3p and Kss1p control G1 arrest in *Saccharomyces cerevisiae* through a balance of distinct arrest and proliferative functions that operate in parallel with Far1p. *Genetics* 151, 989–1004.
- Chou S, Huang L, Liu H (2004). Fus3-regulated Tec1 degradation through SCFCdc4 determines MAPK signaling specificity during mating in yeast. *Cell* 119, 981–990.
- Cosma MP, Panizza S, Nasmyth K (2001). Cdk1 triggers association of RNA polymerase to cell cycle promoters only after recruitment of the mediator by SBF. *Mol Cell* 7, 1213–1220.
- Costanzo M, Nishikawa JL, Tang X, Millman JS, Schub O, Breitkreuz K, Dewar D, Rupes I, Andrews B, Tyers M (2004). CDK activity antagonizes Whi5, an inhibitor of G1/S transcription in yeast. *Cell* 117, 899–913.
- Costanzo M, Schub O, Andrews B (2003). G1 transcription factors are differentially regulated in *Saccharomyces cerevisiae* by the Swi6-binding protein Stb1. *Mol Cell Biol* 23, 5064–5077.
- Cross FR (1995). Starting the cell cycle: what's the point? *Curr Opin Cell Biol* 7, 790–797.
- Cross FR, Buchler NE, Skotheim JM (2011). Evolution of networks and sequences in eukaryotic cell cycle control. *Philos Trans R Soc Lond B Biol Sci* 366, 3532–3544.
- Cross FR, Schroeder L, Bean JM (2007). Phosphorylation of the Sic1 inhibitor of B-type cyclins in *Saccharomyces cerevisiae* is not essential but contributes to cell cycle robustness. *Genetics* 176, 1541–1555.
- Cross FR, Tinkelenberg AH (1991). A potential positive feedback loop controlling CLN1 and CLN2 gene expression at the start of the yeast cell cycle. *Cell* 65, 875–883.

- Cullen PJ, Sprague GF Jr (2012). The regulation of filamentous growth in yeast. *Genetics* 190, 23–49.
- de Bruin RA, Kalashnikova TI, Chahwan C, McDonald WH, Wohlschlegel J, Yates J 3rd, Russell P, Wittenberg C (2006). Constraining G1-specific transcription to late G1 phase: the MBF-associated corepressor Nrm1 acts via negative feedback. *Mol Cell* 23, 483–496.
- de Bruin RA, Kalashnikova TI, Wittenberg C (2008). Stb1 collaborates with other regulators to modulate the G1-specific transcriptional circuit. *Mol Cell Biol* 28, 6919–6928.
- de Bruin RA, McDonald WH, Kalashnikova TI, Yates J 3rd, Wittenberg C (2004). Cln3 activates G1-specific transcription via phosphorylation of the SBF bound repressor Whi5. *Cell* 117, 887–898.
- Dirick L, Nasmyth K (1991). Positive feedback in the activation of G1 cyclins in yeast. *Nature* 351, 754–757.
- Dohlman HG, Thorner JW (2001). Regulation of G protein-initiated signal transduction in yeast: paradigms and principles. *Annu Rev Biochem* 70, 703–754.
- Doncic A, Falleur-Fettig M, Skotheim JM (2011). Distinct interactions select and maintain a specific cell fate. *Mol Cell* 43, 528–539.
- Donovan JD, Toyn JH, Johnson AL, Johnston LH (1994). P40SDB25, a putative CDK inhibitor, has a role in the M/G1 transition in *Saccharomyces cerevisiae*. *Genes Dev* 8, 1640–1653.
- Eriksson PR, Ganguli D, Clark DJ (2011). Spt10 and Swi4 control the timing of histone H2A/H2B gene activation in budding yeast. *Mol Cell Biol* 31, 557–572.
- Escote X, Zapater M, Clotet J, Posas F (2004). Hog1 mediates cell-cycle arrest in G1 phase by the dual targeting of Sic1. *Nat Cell Biol* 6, 997–1002.
- Eser U, Falleur-Fettig M, Johnson A, Skotheim JM (2011). Commitment to a cellular transition precedes genome-wide transcriptional change. *Mol Cell* 43, 515–527.
- Frolov MV, Dyson NJ (2004). Molecular mechanisms of E2F-dependent activation and pRB-mediated repression. *J Cell Sci* 117, 2173–2181.
- Gartner A, Jovanovic A, Jeoung DI, Bourlat S, Cross FR, Ammerer G (1998). Pheromone-dependent G1 cell cycle arrest requires Far1 phosphorylation, but may not involve inhibition of Cdc28-Cln2 kinase, in vivo. *Mol Cell Biol* 18, 3681–3691.
- Geymonat M, Spanos A, Wells GP, Smerdon SJ, Sedgwick SG (2004). Clb6/Cdc28 and Cdc14 regulate phosphorylation status and cellular localization of Swi6. *Mol Cell Biol* 24, 2277–2285.
- Goranov AI, Cook M, Rიცოვა M, Ben-Ari G, Gonzalez C, Hansen C, Tyers M, Amon A (2009). The rate of cell growth is governed by cell cycle stage. *Genes Dev* 23, 1408–1422.
- Haase SB, Reed SI (2002). Improved flow cytometric analysis of the budding yeast cell cycle. *Cell Cycle* 1, 132–136.
- Hartwell LH (1973). Synchronization of haploid yeast cell cycles, a prelude to conjugation. *Exp Cell Res* 76, 111–117.
- Hartwell LH, Culotti J, Pringle JR, Reid BJ (1974). Genetic control of the cell division cycle in yeast. *Science* 183, 46–51.
- Huang D et al. (2009). Dual regulation by pairs of cyclin-dependent protein kinases and histone deacetylases controls G1 transcription in budding yeast. *PLoS Biol* 7, e1000188.
- Jeoung DI, Oehlen LJ, Cross FR (1998). Cln3-associated kinase activity in *Saccharomyces cerevisiae* is regulated by the mating factor pathway. *Mol Cell Biol* 18, 433–441.
- Koch C, Moll T, Neuberger M, Ahorn H, Nasmyth K (1993). A role for the transcription factors Mbp1 and Swi4 in progression from G1 to S phase. *Science* 261, 1551–1557.
- Koch C, Schleiffer A, Ammerer G, Nasmyth K (1996). Switching transcription on and off during the yeast cell cycle: Cln/Cdc28 kinases activate bound transcription factor SBF (Swi4/Swi6) at start, whereas Clb/Cdc28 kinases displace it from the promoter in G2. *Genes Dev* 10, 129–141.
- Koivomagi M, Valk E, Venta R, Iofik A, Lepiku M, Balog ER, Rubin SM, Morgan DO, Loog M (2011). Cascades of multisite phosphorylation control Sic1 destruction at the onset of S phase. *Nature* 480, 128–131.
- Longtine MS 3rd, McKenzie A, Demarini DJ, Shah NG, Wach A, Brachet A, Philippsen P, Pringle JR (1998). Additional modules for versatile and economical PCR-based gene deletion and modification in *Saccharomyces cerevisiae*. *Yeast* 14, 953–961.
- Madhani HD, Galitski T, Lander ES, Fink GR (1999). Effectors of a developmental mitogen-activated protein kinase cascade revealed by expression signatures of signaling mutants. *Proc Natl Acad Sci USA* 96, 12530–12535.
- Morgan DO (2007). *The Cell Cycle: Principles of Control*, London: New Science Press.
- Nash P, Tang X, Orlicky S, Chen Q, Gertler FB, Mendenhall MD, Sicheri F, Pawson T, Tyers M (2001). Multisite phosphorylation of a CDK inhibitor sets a threshold for the onset of DNA replication. *Nature* 414, 514–521.
- Oehlen LJ, Cross FR (1994). G1 cyclins CLN1 and CLN2 repress the mating factor response pathway at Start in the yeast cell cycle. *Genes Dev* 8, 1058–1070.
- Oehlen LJ, Jeoung DI, Cross FR (1998). Cyclin-specific START events and the G1-phase specificity of arrest by mating factor in budding yeast. *Mol Gen Genet* 258, 183–198.
- Pardee AB (1974). A restriction point for control of normal animal cell proliferation. *Proc Natl Acad Sci USA* 71, 1286–1290.
- Peter M, Gartner A, Horecka J, Ammerer G, Herskowitz I (1993). FAR1 links the signal transduction pathway to the cell cycle machinery in yeast. *Cell* 73, 747–760.
- Peter M, Herskowitz I (1994). Direct inhibition of the yeast cyclin-dependent kinase Cdc28-Cln by Far1. *Science* 265, 1228–1231.
- Queralt E, Igual JC (2003). Cell cycle activation of the Swi6p transcription factor is linked to nucleocytoplasmic shuttling. *Mol Cell Biol* 23, 3126–3140.
- Rothstein R (1991). Targeting, disruption, replacement, and allele rescue: integrative DNA transformation in yeast. *Methods Enzymol* 194, 281–301.
- Schwab M, Lutum AS, Seufert W (1997). Yeast Hct1 is a regulator of Clb2 cyclin proteolysis. *Cell* 90, 683–693.
- Schwob E, Bohm T, Mendenhall MD, Nasmyth K (1994). The B-type cyclin kinase inhibitor p40SIC1 controls the G1 to S transition in *S. cerevisiae*. *Cell* 79, 233–244.
- Sherman F (2002). Getting started with yeast. *Methods Enzymol* 350, 3–41.
- Sherr CJ, Roberts JM (1999). CDK inhibitors: positive and negative regulators of G1-phase progression. *Genes Dev* 13, 1501–1512.
- Sidorova JM, Mikesell GE, Breeden LL (1995). Cell cycle-regulated phosphorylation of Swi6 controls its nuclear localization. *Mol Biol Cell* 6, 1641–1658.
- Sikorski RS, Hieter P (1989). A system of shuttle vectors and yeast host strains designed for efficient manipulation of DNA in *Saccharomyces cerevisiae*. *Genetics* 122, 19–27.
- Skotheim JM, Di Talia S, Siggia ED, Cross FR (2008). Positive feedback of G1 cyclins ensures coherent cell cycle entry. *Nature* 454, 291–296.
- Strickfaden SC, Winters MJ, Ben-Ari G, Lamson RE, Tyers M, Pryciak PM (2007). A mechanism for cell-cycle regulation of MAP kinase signaling in a yeast differentiation pathway. *Cell* 128, 519–531.
- Takahata S, Yu Y, Stillman DJ (2009). The E2F functional analogue SBF recruits the Rpd3(L) HDAC, via Whi5 and Stb1, and the FACT chromatin reorganizer, to yeast G1 cyclin promoters. *EMBO J* 28, 3378–3389.
- Thomas BJ, Rothstein R (1989). Elevated recombination rates in transcriptionally active DNA. *Cell* 56, 619–630.
- Tyers M (1996). The cyclin-dependent kinase inhibitor p40SIC1 imposes the requirement for Cln G1 cyclin function at Start. *Proc Natl Acad Sci USA* 93, 7772–7776.
- Tyers M, Futcher B (1993). Far1 and Fus3 link the mating pheromone signal transduction pathway to three G1-phase Cdc28 kinase complexes. *Mol Cell Biol* 13, 5659–5669.
- Valdivieso MH, Sugimoto K, Jahng KY, Fernandes PM, Wittenberg C (1993). FAR1 is required for posttranscriptional regulation of CLN2 gene expression in response to mating pheromone. *Mol Cell Biol* 13, 1013–1022.
- van den Heuvel S, Dyson NJ (2008). Conserved functions of the pRB and E2F families. *Nat Rev Mol Cell Biol* 9, 713–724.
- Visintin R, Prinz S, Amon A (1997). CDC20 and CDH1: a family of substrate-specific activators of APC-dependent proteolysis. *Science* 278, 460–463.
- Wagner MV, Smolka MB, de Bruin RA, Zhou H, Wittenberg C, Dowdy SF (2009). Whi5 regulation by site specific CDK-phosphorylation in *Saccharomyces cerevisiae*. *PLoS One* 4, e4300.
- Wang H, Carey LB, Cai Y, Wijnen H, Futcher B (2009). Recruitment of Cln3 cyclin to promoters controls cell cycle entry via histone deacetylase and other targets. *PLoS Biol* 7, e1000189.
- Wijnen H, Futcher B (1999). Genetic analysis of the shared role of CLN3 and BCK2 at the G(1)-S transition in *Saccharomyces cerevisiae*. *Genetics* 153, 1131–1143.
- Wijnen H, Landman A, Futcher B (2002). The G(1) cyclin Cln3 promotes cell cycle entry via the transcription factor Swi6. *Mol Cell Biol* 22, 4402–4418.
- Wirt SE et al. (2010). G1 arrest and differentiation can occur independently of Rb family function. *J Cell Biol* 191, 809–825.
- Wittenberg C, Reed SI (2005). Cell cycle-dependent transcription in yeast: promoters, transcription factors, and transcriptomes. *Oncogene* 24, 2746–2755.
- Wittenberg C, Sugimoto K, Reed SI (1990). G1-specific cyclins of *S. cerevisiae*: cell cycle periodicity, regulation by mating pheromone, and association with the p34CDC28 protein kinase. *Cell* 62, 225–237.
- Zimmerman ZA, Kellogg DR (2001). The Sda1 protein is required for passage through start. *Mol Biol Cell* 12, 201–219.

Supplemental Materials

Molecular Biology of the Cell

Pope et al.

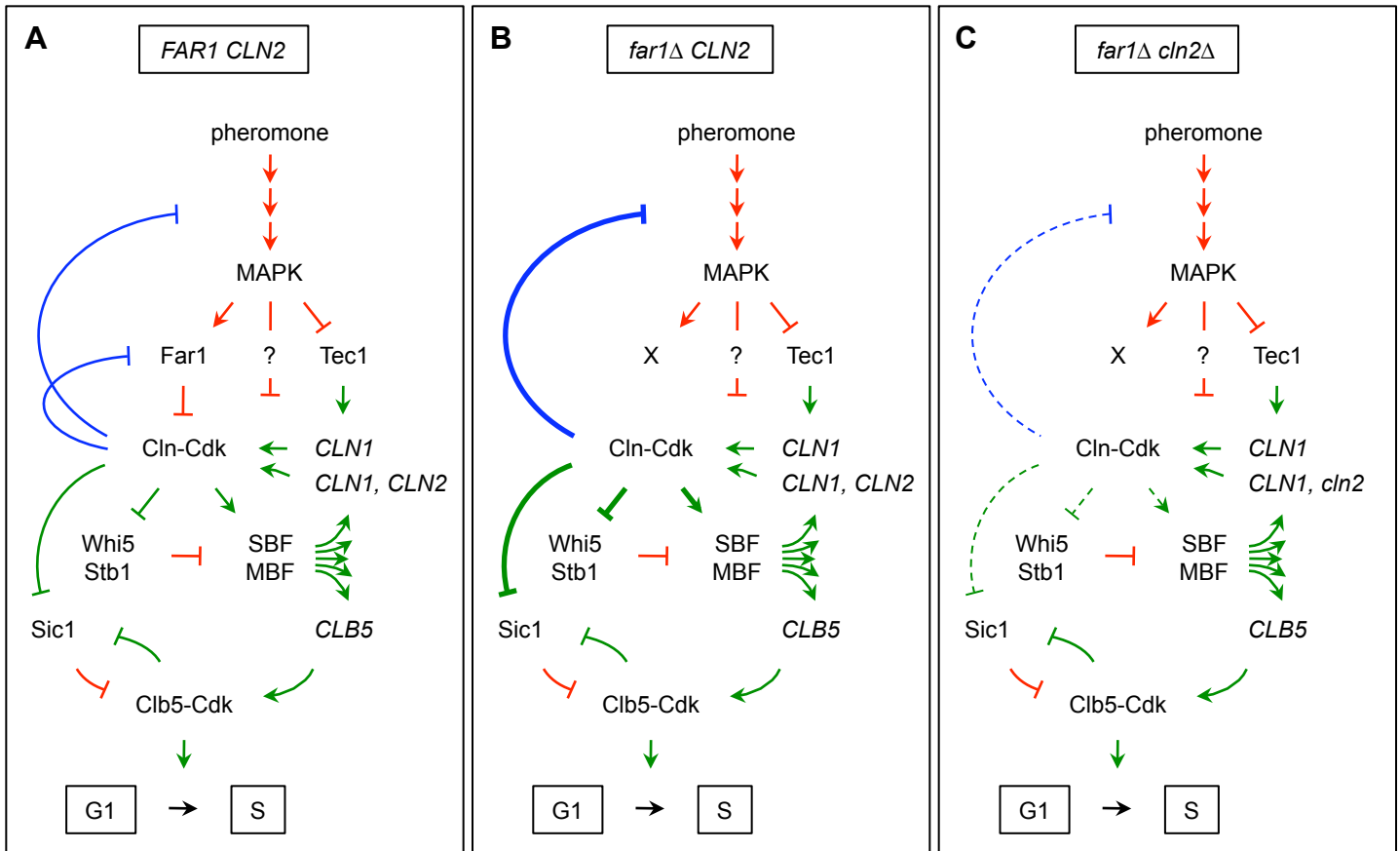


Figure S1. Detailed illustration of regulatory pathways contributing to either pheromone arrest or cell cycle entry.

As in Figure 8, regulatory effects that inhibit or promote the G1/S transition are indicated in red or green, respectively. In addition, inhibitory effects of Cln-Cdk activity on the pheromone pathway are indicated in blue. The question marks indicate that, in addition to regulating Far1 and Tec1, the pheromone-activated MAPK may cause post-translational effects that interfere with the synthesis and/or stability of cyclin proteins (see Discussion).

(A) The pheromone pathway and the cell cycle are mutually antagonistic. In wild-type cells, the ability of pheromone to cause G1 arrest is likely dependent on whether the pheromone signal is received prior to the accumulation of Cln-Cdk activity.

(B) In *far1Δ CLN2* cells, uninhibited Cln-Cdk can more potently drive events that promote the G1/S transition (green arrows) and that inhibit pheromone signaling (blue inhibitory arrow), resulting in resistance to pheromone arrest.

(C) In *far1Δ cln2Δ* cells, the loss of Cln2-Cdk activity can allow other pheromone-induced effects to effectively antagonize the G1/S transition, in a manner dependent on Tec1 destruction and the activities of Whi5/Stb1 and Sic1.